Journal Pre-proof

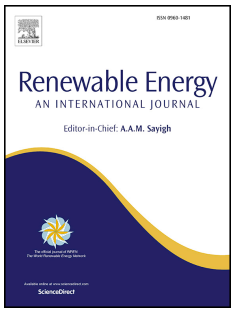

Influence of surface acidity/basicity of selected metal oxide catalysts and reaction atmospheres on the ketonisation of propionic acid to produce 3-pentanone as a liquid biofuel precursor

Abarasi Hart, Himanshu Patel, Eyup Yildirir, Jude A. Onwudili

PII: S0960-1481(25)01048-1

DOI: https://doi.org/10.1016/j.renene.2025.123386

Reference: RENE 123386

To appear in: *Renewable Energy*

Received Date: 7 February 2025

Revised Date: 3 May 2025

Accepted Date: 5 May 2025

Please cite this article as: Hart A, Patel H, Yildirir E, Onwudili JA, Influence of surface acidity/basicity of selected metal oxide catalysts and reaction atmospheres on the ketonisation of propionic acid to produce 3-pentanone as a liquid biofuel precursor, *Renewable Energy*, https://doi.org/10.1016/j.renene.2025.123386.

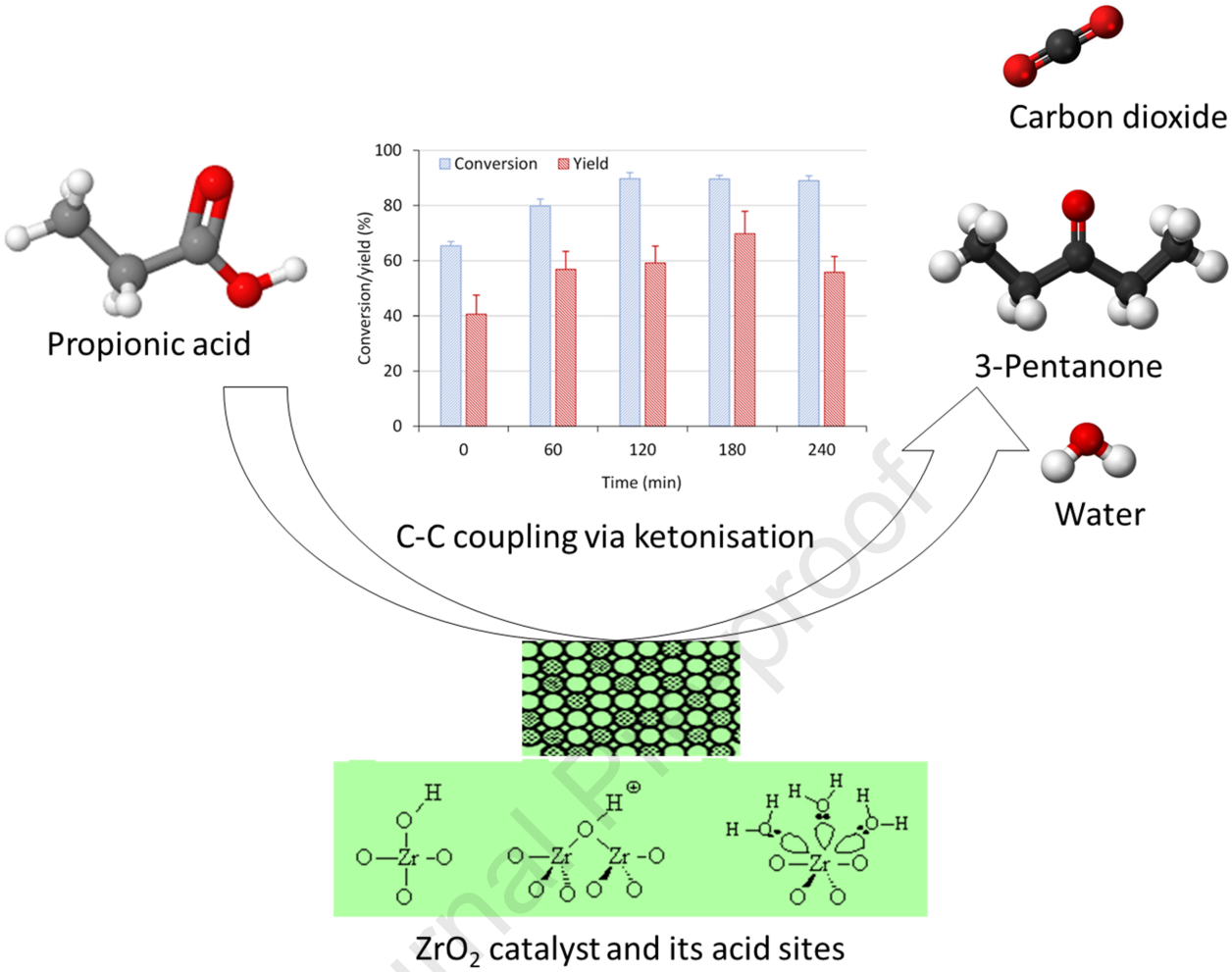

ZrO_2 catalyst and its acid sites

Influence of surface acidity/basicity of selected metal oxide catalysts and reaction atmospheres on the ketonisation of propionic acid to produce 3-pentanone as a liquid biofuel precursor

Abarasi Hart, Himanshu Patel, Eyup Yildirir, and Jude A. Onwudili*

Energy and Bioproducts Research Institute, College of Engineering and Physical Sciences, Aston University, Aston Triangle, Birmingham B4 7ET, United Kingdom

Abstract

Defossilisation of the transportation sector can be achieved via the conversion of renewable biomass into drop-in liquid hydrocarbon-rich fuels. Bio-oils from the pyrolysis of lignocellulosic biomass contain significant proportion of carboxylic acids, which can be upgraded to liquid fuel range precursors via C-C coupling e.g. via ketonisation. In this present study, ZrO_2, SiO_2, and SiO_2–ZrO_2 were synthesised and used for the ketonisation of propionic acid to 3-pentanone, in a stirred 100 mL batch reactor between 300 °C and 400 °C under 10 bar pressure of nitrogen or hydrogen. The order of ketonisation activity by the catalysts was: ZrO_2 > SiO_2–ZrO_2 > SiO_2 under both nitrogen and hydrogen atmospheres, based on their different surface acidity/basicity properties. Under nitrogen, ZrO2 catalyst showed high activity and selectivity towards 3-pentanone with the highest yield of 70.3% at 350 °C. Interestingly, the catalyst gave 12.2% higher yield of 3-pentanone under hydrogen than under nitrogen. This indicated positive influence of hydrogen towards the ketonisation reaction, possibly by preventing formation of intermediates and thus enhancing catalyst stability. Preliminary tests involving mixtures of propionic acid, and a bio-oil sample shows that ZrO_2 was still selective toward ketonisation in the presence of other classes of compounds in bio-oils.

Keywords: Biomass, Pyrolysis bio-oils; Propionic acid; Ketonisation; C-C coupling; Sustainable liquid hydrocarbon fuels

Corresponding Author (j.onwudili@aston.ac.uk)

1. Introduction

Non-edible lignocellulosic biomass such as agricultural waste and forestry residues are regarded as the most sustainable resources to produce carbon-based fuels and organic chemicals. With their abundance, this category of biomass can offer a low-carbon pathway to defossilising the transportation sector, especially the aviation industry, in response to growing climate change concerns. The potential of biomass-derived fuels contributing to the attainment of the UN Sustainable Development Goals (SDGs) through the mitigation of climate change and provision of sustainable and clean energy solutions cannot be overemphasised. Using pyrolysis technology, lignocellulosic biomass can be converted into high yields of bio-oils when heated in the absence of air or oxygen. Bio-oils exhibit elevated levels of oxygenated organic compounds and water contents, from the original oxygen atoms in the biomass feedstock. These oxygenated compounds, primarily comprising of phenolics, carboxylic acids, esters, alcohols, furanics, and others, can be linked to the low thermal and storage stability, low heating value, high viscosity and high acidity of bio-oils. These properties such as corrosiveness [1], poor miscibility with conventional fuels [2], and low calorific value and high viscosity [3], pose significant challenge to the direct application of bio-oils as substitute transportation fuels.

In addition, the organic molecules found in bio-oils have short carbon chain length, which means that their conversion to drop-in liquid hydrocarbons within the range of conventional transportation fuels such as gasoline, kerosene and diesel would require further processing. Important chemistries to achieve this include 1) oxygen removal (deoxygenation) to increase energy density, and 2) carbon chain (C-C) elongation to control molecular weights [4]. Hence, the selection of process conditions and catalyst for bio-oil upgrading process needs to favour deoxygenation and promote C-C chain elongation. Hence, carbon chain elongation reactions such as ketonisation, aldol condensation, Diels-Alder reaction and alkylation are important in this case. However, the multicomponent complexity of bio-oil impedes the mechanistic insight into such complex reaction networks that would result in the

required C-C coupling. Consequently, studies to elucidate reaction mechanisms, optimise process conditions, and develop a robust, stable, and effective catalyst that can selectively activate the pathways to desired final products are usually carried out using relevant model compounds.

Short-chain carboxylic acids such as formic acid, acetic acid and propionic acid is found in pyrolysis bio-oils in substantial quantities [1], contributing to their corrosiveness, instability, and modest energy content [5]. In general, the concentrations of carboxylic acids in bio-oil depend on biomass feedstock [5], and pyrolysis conditions [6]. For example, the concentration of acetic acid can be as high as 17% in beech wood bio-oil [5]. Therefore, the conversion of carboxylic acids in this context, has significant implications for developing biofuels by serving as building blocks for hydrocarbon fuels (C_5-C_{16}) and other chemicals via initial C-C coupling. Ketonisation (or ketonic decarboxylation) is a reaction that converts two carboxylic acid molecules into a longer-chain ketone with carbon dioxide and water as the other products [7], as shown in Equation 1 [8].

$R_1COOH + R_2COOH \rightarrow R_1COR_2 + CO_2 + H_2O$----------Equation 1

Where R_1, R_2 represents an alkyl group.

This reaction concurrently removes oxygen as carbon dioxide and water [7], while converting highly reactive carboxylic functional groups into more chemically stable ketones with elongated C-C chain [9]. As a solvent-free and additives-free reaction, ketonisation of short-chain carboxylic acids partially deoxygenate them into elongated ketones [7], which serves as a precursor for further chain elongation via aldol condensation reaction and subsequent hydrodeoxygenation to liquid hydrocarbon fuel range compounds [1]. This is a clean, promising, and favourable pathway for bio-oil upgrading [10]. The resultant ketone product can act as building block for aldol condensation C-C coupling reaction to further increase the carbon chain length if desired. For all these to be achieved, catalyst development would play a vital role in selectively activating and promoting these target reactions. Considerable

research has gone into developing of catalysts, mainly metal oxides, that can activate ketonisation of carboxylic acids. For example, Gliński et al.[11] reported the screening of catalysts, comprising of oxides (including low lattice energy oxides and amphoteric oxides) of 26 different metals for the ketonisation of propionic acid at temperature ranging from 325 °C to 450 °C. Their results showed that compared with the single oxides, the use of mixed oxides did not produce any significant synergistic effects towards improving the yields of 2-pentanone.

Gürbüz et al.[9] investigated a double fixed-bed system of ketonisation and aldol condensation/hydrogenation reactions in a single reactor using a feed mixture of 20 mol% of butanoic acid in 2-hexanone. The first stage ketonisation was carried out over $Ce_1Zr_1O_x$ catalyst placed on silica granules, giving butanoic acid conversion of 100% with only 11% selectivity towards 4-heptanone at 350 °C, 5 bar, and weight hourly space velocity (WHSV) 1.92 h^{-1}. Consequently, aldol condensation/hydrogenation was attempted simultaneously over Pd/ZrO_2 catalyst placed downstream the single fixed-bed reactor with a double bed system at temperatures of 350 °C, pressure of 5 bar (hydrogen) and liquid flow rate of 0.16 $mL.min^{-1}$, [9]. The result showed that the conversion of 2-hexanone over 0.25 wt% Pd/ZrO_2 was 75% and 45% selectivity towards C_{12} products. In another study with acetic acid, a variety of rare earth metals oxides catalysts were explored for their ketonisation activity. The highest yields of acetone achieved were with La_2O_3, CeO_2, Pr_6O_{11} and Nd_2O_3 [12]. While the highest conversion of acetic acid observed was 80%, the selectivity towards acetone was 99.9 % when the reaction temperature was 350 °C with Pr_6O_{11} catalyst. Similar results were observed during the investigation of Al_2O_3, TiO_2, and CeO_2 catalysts for both adsorption and catalytic reaction of gas-phase acetic acid at temperatures between 300 °C and 400 °C [13]. Acetone was the dominant product when ceria and titania were present [13]. Additionally, it was found that increasing the reaction time could lead to further deoxygenation and metathesis to produce gases like isobutene and methane.

Moreover, Lee et al. [14] screened MgO, MnO_x, Al_2O_3, TiO_2, ZrO_2, CeO_2, and Si_xAl_yO as heterogeneous catalysts for the ketonisation of hexanoic acid at a temperature of 360 °C and weight-hourly space velocity of 4 h^{-1}. Using 0.2 g loading of each catalyst, the authors reported the production of fuel relevant 6-undecanone [14]. The results showed that MgO and MnO_x gave hexanoic acid conversions of 62% and 75.8%, while the selectivity towards 6-undecanone was 87.5% and 92.6%, respectively. The authors further observed that although, the basic catalysts MgO and MnO_x demonstrated considerable catalytic activity, their leaching in the presence of the acidic reactant could lead to deactivation over time [14]. Furthermore, ketonisation of propionic acid to yield 3-pentanone was investigated over CeO_2-based and composite oxides of CeO_2–MO_x (M = Mg, Al, Cr, Mn, Fe, Co, Ni, Cu, and Zr) using a fixed bed flow reactor at a temperatures range of 300–425 °C under the atmospheric pressure of nitrogen (flow rate of 40 cm^3min^{-1}) and liquid flow rate of 2 ml h^{-1} [10]. The results showed that CeO_2–Mn_2O_3 catalyst produced the highest propionic acid conversion of 73.9% and selectivity towards 3-pentanone was 97.4%, while the addition of Mg, Fe, Ni, Cu, and Zr into CeO_2 decreased selectivity towards the ketone product.

From these ketonisation studies, notable catalysts were mostly amphoteric oxides such as CeO_2, TiO_2, ZrO_2 and MnO_2, which gave high yields of corresponding ketones [11], [15]. However, formation of undesirable products and catalyst deactivation remain important challenges, especially with deactivation attributed adsorption of unreactive intermediate species (leading to coking) and structural disintegration. Recent work by Wang and Iglesia [16], showed that deactivation of metal oxide catalysts during ketonisation could be inhibited using transition metals such as Cu/SiO_2 as co-catalyst to convert problematic intermediates. The authors claimed that catalytic hydrogenation of undesirable intermediates was key to the enhanced catalyst stability and yields of ketonisation products [16]. However, information on how the acidity and basicity properties of metal oxide catalysts influences carboxylic acid ketonisation is limited in the literature. This present study investigated the effect of surface acidity/basicity properties of metal oxide catalysts on the ketonisation of propionic acid as model compound for C-C coupling of carboxylic acids during bio-oil

upgrading to conventional fuels. Biomass-derived propionic acid for 3-pentanone production offers the following benefits 60% reduced greenhouse gas emissions and environmental impact [17], cost-effective and direct production method (e.g., pyrolysis, etc.), sustainable production, and carbon-neutrality, as opposed to fossil-based sources [18]. Additionally, it provides a transition pathway to renewable energy and sustainable biomass management strategy. Furthermore, biomass-derived propionic acid can serve as a building block for the chemical industry and its production can also be integrated into biorefinery, allowing the production of multiple bioproducts from the same biomass feedstock [17].

Catalysts play a critical role in promoting sustainable and eco-friendly chemical reactions. Based on the reviewed literature, most studies used either acidic or basic metal oxides catalysts for converting carboxylic acids to ketones. So, the choice of ZrO_2 and SiO_2 allows the effect of highly amphoteric, mixed acidic/basic and weak acidic metal oxides catalysts to be comparatively evaluated. Additionally, zirconia (ZrO_2) and silica (SiO_2) can withstand chemical degradation in severe and acidic reaction conditions, ensuring long-term catalytic effectiveness [19]. Furthermore, the development of robust, low-cost, and easy-to-prepare catalysts is crucial for both industrial-scale and sustainable applications. While, in this case, ZrO_2, SiO_2 and their mixtures were synthesised, characterised and used to catalyse the solvent-free liquid phase ketonisation of propionic acid under hydrogen and nitrogen atmospheres. Most published studies are vapour/gas phase ketonisation of short chain carboxylic acids, liquid phase is less investigated. The influence of the different acidity/basicity properties of the catalyst on feedstock conversion and ketone yields were measured in relation to reaction temperature and reaction times. Also, investigated is the effect of bio-oil compounds on the ketonisation of propionic acid at the optimum reaction temperature, time and atmosphere (H_2) using 50/50 mixture of propionic acid and bio-oil. Additionally, the stability of the catalysts under different reaction atmospheres were evaluated to determine their performance and potential for further optimisation. Results from this work would contribute to the deployment of sustainable liquid transportation fuels via pyrolysis bio-oil upgrading.

2. Materials and methods

2.1 Materials

Analytical grade propionic acid, 3-pentanone, acetone, zirconyl chloride octahydrate ($ZrOCl_2 \cdot 8H_2O$), sodium meta-silicate nanohydrate ($Na_2SiO_3.9H_2O$), hydrochloric acid (HCl), and 50 % vol/vol aqueous solution of ammonium hydroxide (NH_4OH) were all purchased from Fisher Scientific, Leicester, UK and used as received. The propionic acid was used as feedstock for the reaction, 3-pentanone was used to prepare calibration curve for its quantification in the reaction products and acetone was used as solvent for the preparation of standard solutions for analysis. The hydrate salts were used as precursors for the preparation of the respective catalysts.

2.2 Catalyst synthesis

The ZrO_2 and SiO_2 catalysts were prepared by precipitation method. 40 g of each precursor was dissolved in 400 mL deionized water. For the synthesis of ZrO_2, aqueous solution of NH_4OH was added dropwise to the solution of $ZrOCl_2.8H_2O$ until the pH is in the range of 9-10, while HCl was utilised for $Na_2SiO_3.9H_2O$ solution to attain pH of 8-9. The suspension was mixed vigorously at 60 °C for 6 h and aged for 24 h. The solutions were aged at 60 °C for 6 h, repeatedly rinsed with distilled water until the solution shows a pH of 7 at which acid and residual chlorine have been removed, then filtered and oven-dried at 105 °C for 12 h. The calcination of the samples was carried out at 500 °C for 4 h at a heating rate of 10 °C/min. The mixed oxides (ZrO_2-SiO_2) catalyst was prepared with the same method by co-precipitation at a ratio of 1:1. In terms of the catalyst stability, after each experiment, the catalyst was recovered washed with acetone and dried at 95 °C for 6 h and then reused for repeated experiment. At the end of the third cycle of repeated experiment, the catalyst was regenerated via oxidation in air atmosphere at 500 °C for 2 h.

185 **2.3 Catalyst characterisation**

186 The physico-chemical properties of the synthesised catalysts which connects their
187 performance and activity were determined through material characterisation techniques that have
188 been previously reported in the research group [17]. Briefly, the catalysts pore sizes and specific
189 surface areas were determined through nitrogen-physisorption technique (Quantachrome
190 Instruments NOVA 4200), while their bulk crystal structure, crystallinity, and phase composition were
191 analysed using X-ray diffraction (XRD) technique (Bruker D8 Advance A25). The acid site types, and
192 strength were determined and quantified by pyridine Fourier-transform infrared (pyridine-FTIR)
193 spectroscopy. This is based on the adsorption of pyridine on the acid sites of catalyst, which was
194 recorded using Nicolet iS50 FTIR Spectrometer, ThermoFisher Scientific at a resolution of 4 cm^{-1}. The
195 content of coke and residues deposited on the spent ZrO_2 catalyst after ketonisation was studied using
196 thermogravimetric analyser (TGA) method (TGA/DSC 2 STAR^e System, Mettler-Toledo). The method
197 applied for the analysis is tramp temperature from 40 to 900 °C at the rate of 10 °C/min, and
198 isothermal condition at 900 °C for 15 min using an air flowing rate of 30 cm^3/min.

199

200 **2.4 Experimental procedure for ketonisation**

201 For each experiment, 15 g of propionic acid, along with 1.0 g of ZrO_2 catalyst, were introduced into a
202 100 mL stirred batch reactor procured from Parr Instrument Company, IL, USA. The batch reactor was
203 equipped with a motor-powered impeller, a thermocouple, a 1 kW electric heater, a temperature
204 controller with thermocouple, a water-cooled solenoid, a digital pressure readout, and a standard
205 pressure gauge. The reactor was subsequently sealed, pressurized to 10 bar with either N_2 or H_2, and
206 heated to the designated temperature at an average rate of 12 °Cmin^{-1} and stirring speed of 500 rpm.
207 Once the set temperature (300 - 400 °C) was reached, it was maintained constant throughout the
208 designated reaction time. At the end of the reaction, the reactor was cooled with the help of a fan,
209 reaching 50 °C in less than 15 minutes.

210 **2.5 Analysis of products**

211 Each experiment produced gas, liquid, and solid products whereas the solid component comprised
212 spent catalyst and solid residue from the feedstock (char). Whereas the gas composition was
213 determined by sampling into a 1-L Tedlar gas bag and injecting it into a Shimadzu GC-2014 gas
214 chromatograph equipment fitted with thermal conductivity and flame ionization detectors (TCD &
215 FID). The analytical methodology for gas analysis has been previous reported elsewhere [2]. The
216 amount of gas produced was quantified using ideal gas equation relating pressure, volume, and
217 temperature data after the reactor was cooled down post-experiment. The solid residue after the
218 reaction was filtered and dried at 105 °C for 6 h. The amount of char produced from the reaction was
219 estimated by weighing the dried solid and subtracting the initial mass of the catalyst.
220
221 The compositions of the organic liquid products were analysed using gas chromatograph/mass
222 spectrometer (GC/MS). Specifically, a Shimadzu GC-2010 Plus gas chromatograph equipped with a
223 Shimadzu mass spectrometer (model QP2010 SE) was employed. The mass selective detector
224 operated in the electron impact (EI) ionisation mode. For separation, a 30 m long column with a
225 diameter of 0.25 mm (SH-Rtx-5MS) supplied by Thames Restek, UK, was used. Oven temperature was
226 held at 40 °C for 6 min, then ramped at 3 °C/min to 180 °C. Subsequently, the heating rate was
227 increased to 10 °C/min until the temperature reached 280 °C, marking the completion of the analysis.
228 Additionally, calibration curves of the GC-MS for propionic acid and 3-pentanone were prepared to
229 quantify these chemicals to determine conversions, yields, and selectivities after each experiment.
230 Five different (20, 40, 60, 80, and 100 µL of propionic acid/3-pentanone per 1.6 mL acetone) vol/vol
231 ratios of each chemical were prepared injected into the GC-MS to calculate the response factors and
232 prepare a calibration curve. The conversion of propionic acid following self-ketonisation reaction is
233 calculated using Equation 2, while the yield of 3-pentanone the desired product is calculated using
234 Equation 3.

$$Conversion\ [\%] = \frac{Moles_{PPi} - Moles_{PPf}}{Moles_{PPi}} \times 100 \qquad \text{(Equation 2)}$$

$$Product\ yield\ [\%] = \frac{Moles_{3PT}}{Moles_{PPi}} \times 100 \qquad \text{(Equation 3)}$$

$Moles_{PPi}$ = mole of propionic acid fed into the reactor

$Moles_{PPf}$ = mole of propionic acid recovered after reaction

$Moles_{3PT}$ = mole of 3 − pentanone recovered after reaction

3. Results and discussion

3.1 Product distribution from the ketonisation of propionic acid

3.1.1 Effect of reaction temperature under nitrogen atmosphere

The catalytic ketonisation of propionic acid was carried out under 10 bar bar of N_2 at temperatures between 300 and 400 °C to monitor the effect of reaction temperatures. **Table 1** shows the distribution of gas, liquid, and solid products for ketonisation of propionic acid over SiO_2, ZrO_2- SiO_2 and ZrO_2 catalysts in relation to reaction temperature. In general, mass balance closures of 95 wt% or greater were achieved, showing good accountability of product distributions. In all cases, liquid was the main product except with ZrO_2 at 400 °C, when gas yields surpassed those of liquids due to increased rate of other reactions beyond ketonisation. The results in Table 1 shows that liquid yields decreased as the reaction temperature increased from 300 °C to 400 °C, while the gas yields increased with temperature for both non-catalytic and catalytic reactions. This can be ascribed to the increased

rate of random reactions such as C-C cleavages (pyrolysis) [21], or decarboxylation of the carboxylic acid [22], with increasing reaction temperature. Notably, the reactions at 400 °C produced the highest amount of gas products for each set of reaction as presented in **Table 1**. Compared to non-catalytic experiments, addition of weak acid site oxide SiO_2 catalyst did not change the product distribution significantly while addition of highly amphoteric oxide ZrO_2 highly affected the gas produced from the reaction at 400 °C, making it the main final product.

Table 1. Product distribution during catalytic and non-catalytic reactions of propionic acid under 10 bar N_2 atmosphere with a reaction time of 180 minutes

Catalyst	Temperature [°C]	Solid [g]	Liquid [g]	Gas [g]	Total [g]	Mass Balance [%]
-	300	0.02	13.10	1.62	14.74	98.3
-	350	0.12	9.39	4.80	14.31	95.4
-	400	0.16	8.43	5.86	14.45	96.3
SiO_2	300	0.07	13.65	0.90	14.62	97.5
SiO_2	350	0.20	9.86	4.57	14.63	97.5
SiO_2	400	0.03	8.35	6.16	14.54	96.9
ZrO_2- SiO_2	300	0.12	12.98	1.51	14.61	97.4
ZrO_2- SiO_2	350	0.10	10.11	4.12	14.33	95.5
ZrO_2- SiO_2	400	0.09	8.90	5.28	14.27	95.1
ZrO_2	300	0.45	12.08	1.89	14.42	96.1
ZrO_2	350	0.12	9.67	4.86	14.65	97.7
ZrO_2	400	0.20	5.77	8.27	14.24	94.9

The conversion of propionic acid following reactions in the absence and presence of weak acidic oxide (SiO_2), moderately amphoteric oxide (ZrO_2- SiO_2), and highly amphoteric oxide (ZrO_2) catalysts as a function of reaction temperature under nitrogen atmosphere is shown in **Figure 1**. For the non-

catalytic reactions, the conversion of propionic acid increased as the reaction temperature increased from 300 °C to 400 °C, implying increasing reaction rate with temperature. However, the yield of 3-pentanone increased from 14.2% at 300 °C to 49.9% at 350 °C. Increasing the reaction temperature to 400 °C resulted in a decreased yield to 40.4%. This aligns with the observation reported in Table 1, which shows that gas output increased as the reaction temperature increased from 300 °C to 400 °C, causing a decrease in the yield of the desired product. This result implied that the ketonisation was not solely taking place on the surface of the catalyst [23].

Compared to non-catalytic reactions, the use of weak acidic oxide SiO_2 as catalyst led to significant reduction in propionic acid conversion as well as the yield of 3-pentanone. However, the moderately amphoteric mixed metal oxides of ZrO_2-SiO_2 produced similar yields of 3-pentanone at 350 °C and 400 °C as those achieved for non-catalytic reactions. In contrast, the conversion of propionic acid conversion was substantially lower at the three investigated temperatures with ZrO_2-SiO_2 catalyst relative to those obtained for non-catalytic counterparts. One of the mechanisms reported for ketonisation of carboxylic acids on metal oxide catalysts involves α-C−H cleavage during adsorption and dissociation on the catalyst surface [16]. This would result in 1-hydroxy enolates that pair with adsorbed carbonyl from another acid molecule to create a coupled C−C bond ketone [24].

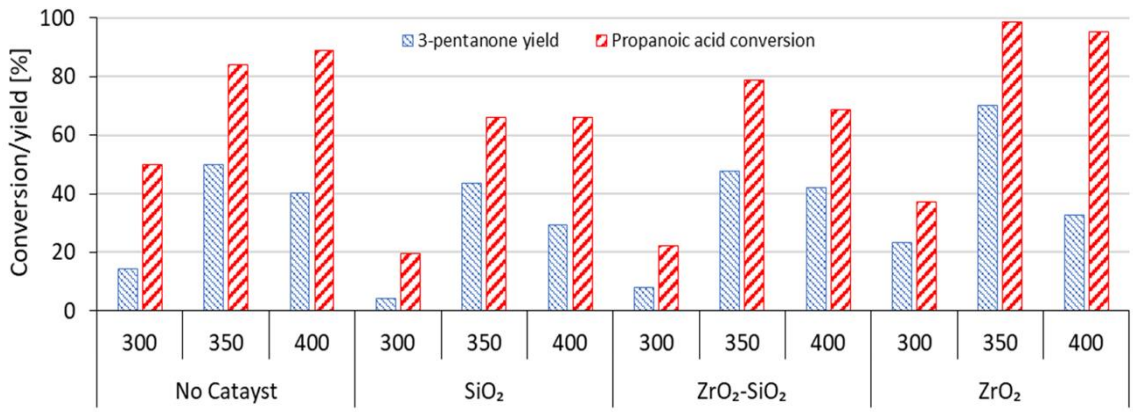

Figure 1. Conversion of propionic acid due to catalytic ketonisation and yield of 3-pentanone for the various synthesised catalysts and reaction temperature under 10 bar nitrogen atmosphere and 180 min reaction time.

When propionic acid ketonisation was carried out with ZrO_2 catalyst, conversion increased from 37.1% to nearly 99% as the reaction temperature increased from 300 °C to 350 °C. Further increase in reaction temperature to 400 °C led to complete conversion of the feed. The conversion obtained at 350 °C in this study with ZrO_2 catalyst was higher than the 92.8% reported for CeO_2–Mn_2O_3 (Mn content of 60 mol%) catalyst in the ketonisation of propionic at the same temperature [10]. For the three temperatures investigated in the present work, the ZrO_2 catalyst accomplished higher conversions than non-catalytic counterpart except for 300 °C. As shown in **Figure 1**, similar conversions of propionic acid and yields of 3-pentanone were achieved at 300 °C, with or without catalyst, indicating that the catalyst was not active at this temperature. The yields of 3-pentanone in the presence of ZrO_2 catalyst were as follows: 23.4% (300 °C), 70.3% (350 °C), and 32.7% (400 °C). These results confirmed that 350 °C reaction temperature was most favourable for the yield of the desired product 3-pentanone. The compositions of compounds in the liquid products from the catalytic and non-catalytic tests were clearly different as shown by GC-MS analysis ***(see Supplementary Information Tables S1 and S2)*.**

This optimum temperature of 350 °C aligned with the optimization study on rare earth metal oxides for the ketonisation of acetic acid to acetone previously reported in the literature [12]. However, the density of basic sites would have been reduced with the doping of ZrO_2 with SiO_2 to form binary oxide of SiO_2-ZrO_2, which decreases the amphoteric strength relative to pure ZrO_2 catalyst [25]. Thus, it can be concluded that highly amphoteric metal oxide ZrO_2 catalyst exhibited a superior activity for propionic acid ketonisation followed by moderate amphoteric mixed oxides ZrO_2-SiO_2 and then weak acidic oxide SiO_2 catalysts. This collaborates with literature that amphoteric metal oxides such as ZrO_2 are known to be more effective for ketonisation of carboxylic acids. Examples include ketonisation studies of propionic acid over CeO_2 catalyst [26], acetic, propionic, and butyric over Ru/TiO_2 catalyst [27], and propionic acid over TS-1 and Ti-Beta zeolites catalysts [28]. Equally, for short-chain propionic acid used as a feedstock in this study, high conversion (99%) and high yield of 3-pentanone (70%) was

320 achieved with ZrO_2 catalyst under similar conditions. In comparison, these were better results than
321 the work reported by Aleem et al. [29], in which ZrO_2 catalysed the ketonisation of long-chain palmitic
322 acid with a conversion of 85% but low palmitone yield of 17% at 340 °C under nitrogen atmosphere
323 using 15 g of feedstock and 0.75 g catalyst loading. Hence, it is plausible that amphoteric metal oxides
324 such as ZrO_2 exhibited higher catalytic activity and selectivity in the ketonisation of short-chain
325 carboxylic acids than long-chain ones.

326 Numerous mechanisms have been proposed for the ketonisation of carboxylic acids [1], [30]. Most
327 reported mechanisms have indicated that the ketonisation reaction is catalysed by Lewis' acid-base
328 pairs on the surface of metal oxides. They include C–C bond formation via 1-hydroxy enolate reactions
329 [16], the presence of a H-atom at an α-position to the –COOH group [24], monodentate carboxylate
330 activated α-H abstraction forming an enolate that acts a nucleophile to attack a co-adsorbed
331 carboxylic acid/carboxylate to produce a β-ketoacid intermediate [26], and α-H abstraction and C-C
332 coupling via a β-ketoacid intermediate [28]. Also, the high lattice energy of ZrO_2 due to the strong
333 metal-oxygen bonds is another contributing factor for its catalytic performance for ketonisation at 350
334 °C [31]. This was due to surface ketonisation which is activated by the varying strengths of acid-base
335 pair sites on the surfaces of the amphoteric metal oxide ZrO_2 catalyst, resulting in different activities
336 leading to the formation and decomposition of carboxylates [1]. Hence, as reported in literature, at
337 350 °C the ketonisation proceeded on the catalyst surface by interaction of two adsorbed molecules
338 of propionic acid [10]. One propionic acid molecule would undergo dissociative adsorption at the
339 catalytic sites, which would cause surface carboxylate species to form. A dianion would then be
340 formed via α-H abstraction from the carboxylate species, according to the mechanism reported by
341 Guo et al. [26]. On reacting with another acyl species produced through dehydroxylation of another
342 propionic acid, the carboxylate species would form the β-ketoacid intermediate and subsequently
343 decomposed to 3-pentanone, CO_2, and water as side products [26]. Clearly, the prevailing mechanism
344 must essentially cause both dehydration and decarboxylation reactions to occur simultaneously
345 between two carboxylic acid molecules. Giving the superior catalytic activities of amphoteric oxides

346 during ketonisation., the critical reactions must rely on the ability of such catalysts to have, (1)
347 sufficient acidity to catalyse the condensation reaction between two carboxylic acid groups leading to
348 loss of one molecule of water (dehydration) while forming an acylium ion and a resonance-stabilised
349 carboxylate ion – carbanion system that is chemisorbed on the metal oxide catalyst; (2) sufficient basic
350 character to stabilise the α-carbon of into a carbanion that can attack the carbonyl carbon of acylium
351 ion. The nucleophilic attack of carbanion on the positive carbon on the acylium ion leads to the
352 formation of a β-keto acid, which undergo decarboxylation to form CO_2 and the resulting ketone
353 product.

354

355 **3.1.2 Effect of reaction time at 350 °C with ZrO_2 under nitrogen atmosphere**

356 In Section 3.1.1, the trade-off between liquid and gas products showed that the optimum yields liquid
357 product and the maximum yield of 3-pentanone (70.3%) were both achieved at 350 °C. Indeed, at
358 temperature of 400 °C most of the propionic acid was converted into gas. These results were achieved
359 by keeping the reaction time constant reaction time at 180 min using nitrogen gas atmosphere. Hence,
360 further experiments were conducted to see the effect of carrying out the reactions with lower reaction
361 times, to possibly reduce its energy demand. Hence, in addition to 180 min, reactions were tested
362 under N_2 atmosphere at reactions times of '0' min to 240 min at 350 °C. Here '0 min' indicated that
363 the reactor was removed from the heater and cooled once the reaction temperature was reached.
364 **Table 2** presents the yields of gas, liquid and solid products from each experiment at reaction ranging
365 from 0 to 240 min under nitrogen atmosphere. The results demonstrated that the mass balances were
366 within 97 wt% or greater. While the liquid product steadily reduced as the reaction time progressed
367 from 0 to 240 min, the solid product increased as the reaction increased from 0 to 120 min and
368 reached a plateau between 120 and 240min. However, the gas yields increased as the reaction
369 proceeded from 0 to 60 min, and remained within an average of 3.6 g for reaction time from 60 to 240

min. This showed that the reaction time significantly affected the yield of liquid product than solid and gas.

While the focus of this research was mainly on the liquid products, **Table 3** shows the compositions of gas products obtained from the reaction of propionic acid at 350 °C for 180 min in the presence of ZrO_2. The gas components included CO_2, CO, H_2, and light hydrocarbon gases (C_1–C_4), with CO_2 as the dominant gas, with a 91.75 wt% in relation to the yield of gas product.

Table 2. Product distribution during ketonisation at different times variations under 10 bar initial pressure at 350 °C with ZrO_2 catalyst.

Time [min]	Reaction atmosphere	Solid [g]	Liquid [g]	Gas [g]	Total [g]	Mass Balance [%]
0	N_2	0.22±0.03	11.85±1.12	2.50±0.91	13.72±0.09	97.13±1.27
60	N_2	0.30±0.02	10.89±0.18	3.53±0.36	14.71±0.19	98.07±0.40
120	N_2	0.31±0.03	10.78±1.19	3.64±1.08	14.73±0.10	98.20±0.67
180	N_2	0.33±0.08	10.68±0.67	3.74±1.03	14.75±0.22	98.32±0.58
240	N_2	0.33±0.02	10.54±0.89	3.62±0.80	14.48±0.13	96.57±0.87

The presence of gases other than CO_2 (reaction Eq. 1) was indicative of the occurrence of other reactions such as decarbonylation (loss of CO), and pyrolysis or thermal cracking (C_1–C_4). However, the formation of CO can be attributed to carbonylation of the produced 3-pentanone. The thermal cracking of the resulting C_3 and C_4 hydrocarbons due to decarboxylation and decarbonylation of propionic acid and 3-pentanone, led to the formation of C_1-C_4 hydrocarbons in the produced gas. The dominant light hydrocarbon gas was ethene, which could be formed from a concerted dehydration and decarbonylation of propionic acid as shown in Equation 4.

$C_2H_5COOH \rightarrow C_2H_4 + CO + H_2O$----------Equation 4

Table 3. Nitrogen-free gas composition for ZrO_2 at 350 °C temperature, 10 bar N_2 initial pressure, and 180 min reaction time.

Gas	ZrO_2 (N_2)
H_2 (wt%)	0.39
CO_2 (wt%)	91.8
CO (wt%)	2.93
CH_4 (wt%)	0.20
C_2H_4 (wt%)	0.64
C_2H_6 (wt%)	3.73
C_3H_6 (wt%)	0.08
C_3H_8 (wt%)	0.13
C_4H_{10} (wt%)	0.16

The conversion of propionic acid and yield of 3-pentanone as a function of reaction time over ZrO_2 catalyst under nitrogen atmosphere is shown in **Figure 2** ***(see Supplementary Information Figure S1 for additional semi-quantitative data)***. The conversion of propionic acid increased from 65.4% to 90% as the reaction increased from 0 to 120 min and remained at approximately 90% as the reaction time was further increased from 120 to 240 min. However, the yield of 3-pentanone increased steadily from 40.5% when the reactor achieved 350 °C temperature to about 69.8% at a reaction time of 180 min. Further increase in reaction time to 240 min resulted in 3-pentanone decline to 55.8%, which corresponded to the decrease in liquid product (Table 2) yield. Therefore, a trade-off between the conversion of propionic acid and yield of 3-pentanone proved the optimum results 90% and 70%, respectively at 180 min reaction time.

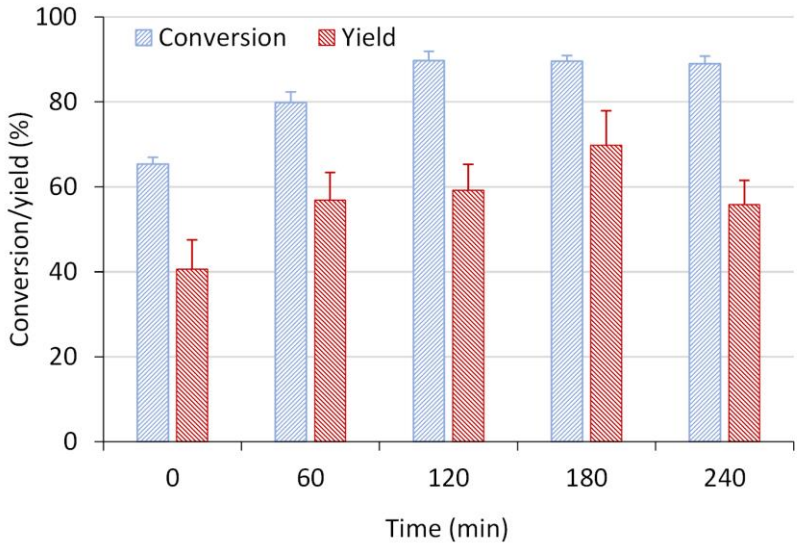

Figure 2. Conversion of propionic acid and yield of 3-pentanone as a function of reaction time over ZrO_2 catalyst at 350 °C temperature, under 10 bar initial nitrogen atmosphere.

3.1.3 Influence of hydrogen atmosphere on the ketonisation of propionic acid

Section 3.1.2 showed that the yields of 3-pentanone was highest at 180 min under nitrogen in the presence of ZrO_2, SiO_2, SiO_2-ZrO_2 catalysts. Hence, the effect of hydrogen on the ketonisation of propionic acid over metal oxide catalysts of vary degree of amphoteric characteristics was investigated at 350 °C, 10 bar H_2, and 180 min (**Table 4**). The results showed that the yield of solid products decreased slightly under hydrogen atmosphere compared to under nitrogen. However, the role of hydrogen atmosphere on the catalyst selectivity towards 3-pentanone seemed to be different. While the liquid and gas products are within a similar range, there is more solid char produced with ZrO_2 than SiO_2 and SiO_2-ZrO_2 catalysts. Notably, the use of hydrogen gas atmosphere in the presence of ZrO_2 suppressed solid formation and slightly increased gas production, while the liquid yield decreased slightly compared to experiments under nitrogen at 350 °C. It has been reported that the presence of hydrogen can minimise coke formation due to the conversion of coke-forming intermediate species on the catalyst surface.

422 **Table 4**. Product distribution during ketonisation under 10 bar H_2 atmosphere with different
423 catalysts at 350 °C for 180 min.

Catalyst	Temperature [°C]	Solid [g]	Liquid [g]	Gas [g]	Total [g]	Mass Balance [%]
-	350	0.10±0.03	11.11±1.20	3.12±0.91	14.33±0.09	95.5±1.27
SiO_2	350	0.05±0.02	9.11±0.18	5.41±0.36	14.57±0.49	97.1±0.40
ZrO_2- SiO_2	350	0.04±0.03	8.92±2.19	5.54±1.08	14.5±0.10	96.7±0.67
ZrO_2	350	0.15±0.02	8.75±0.89	5.41±0.80	14.31±0.13	95.4±0.87

424

425 For ketonisation of propionic acid at 350 °C temperature, 10 bar initial pressure, 1.0 g of ZrO_2 catalyst,
426 and 180 min reaction, the solid yield decreased from 2.2 wt% under nitrogen atmosphere to 0.9 wt%
427 with hydrogen, representing 1.3 wt% reduction in carbon formation with hydrogen (**Tables 2** and **4**).
428 This is further confirmed by the increased gas yield from 25 wt% (nitrogen) to 29.2 wt% (hydrogen)
429 due to hydrogen termination of free radical species (e.g., methyl, ethyl, etc.) from the cleavage of C-C
430 bond. However, the liquid yields are comparable under nitrogen and hydrogen atmosphere.

431

432 **Figure 3** shows the conversion of propionic acid from its reactions in the presence of the SiO_2, ZrO_2-
433 SiO_2, and ZrO_2 catalysts at 350 °C optimum reaction temperature under hydrogen atmosphere. Clearly,
434 the catalytic activity and performance of the highly amphoteric metal oxide ZrO_2 catalyst for the
435 ketonisation of propionic acid at 350 °C to 3-pentanone improved significantly under hydrogen
436 atmosphere relative to nitrogen atmosphere, when **Figures 2** and **3** are compared ***(see also,***
437 ***Supplementary Information Tables S2 and 3)***. Consequently, the conversion and yield of 3-pentanone
438 decreased as the degree of amphoteric nature of the catalysts decreased in the order SiO_2 << ZrO_2-
439 SiO_2 < ZrO_2 (**Figure 3**). One of the plausible reasons for the increased catalytic activity in hydrogen
440 atmosphere can be attributed to metal oxide reduction removing the lattice oxygen. It has been
441 reported that hydrogen adsorption and dissociation on the active sites of the catalyst promoted
442 surface ketonisation [7], with surface catalysis of ketonisation occurring above 300 °C [7]. ZrO_2 catalyst

exhibits amphoteric, oxidizing and reducing properties [25]. The redox and basicity/acidity properties as observed in ZrO_2, Y_2O_3–ZrO_2 and SiO_2–ZrO_2 catalysts [25], the surface lattice oxygen arising from Zr^{4+} ion [32], and the redox properties of ZrO_2 arising from the amphoteric acid-base $Zr^{4+}O^{2-}$ pair enhanced its ketonisation activity towards 3-pentanone [33]. In contrast to nitrogen atmosphere, it has been proposed that the reduction of ZrO_2 under hydrogen atmosphere occurs by the elimination of surface OH-groups [33], due to dissociatively activated hydrogen reacting to produce water [34]. Furthermore, under hydrogen atmosphere, the amphoteric ZrO_2 catalyst could have experienced reduction which is beneficial to the propionic acid ketonisation based on a density functional theory (DFT) analysis of reduced ZrO_2. Based on DFT and experimental studies, it was found that reduction via hydrogen adsorption/water desorption from a hydroxylated surface of the ZrO_2 can occur [35], the reduced ZrO_2 can stabilise the acyl intermediate [36], while oxygen vacancies stabilised the reaction product [37], and significantly lowered the activation energy during ketonisation reaction of carboxylic acid [38]. Hence, the increased catalytic activity of ZrO_2 under hydrogen atmosphere relative to nitrogen can be credited to reduced zirconia surface occurring during ketonisation of propionic acid (**Figures 2** and **3**).

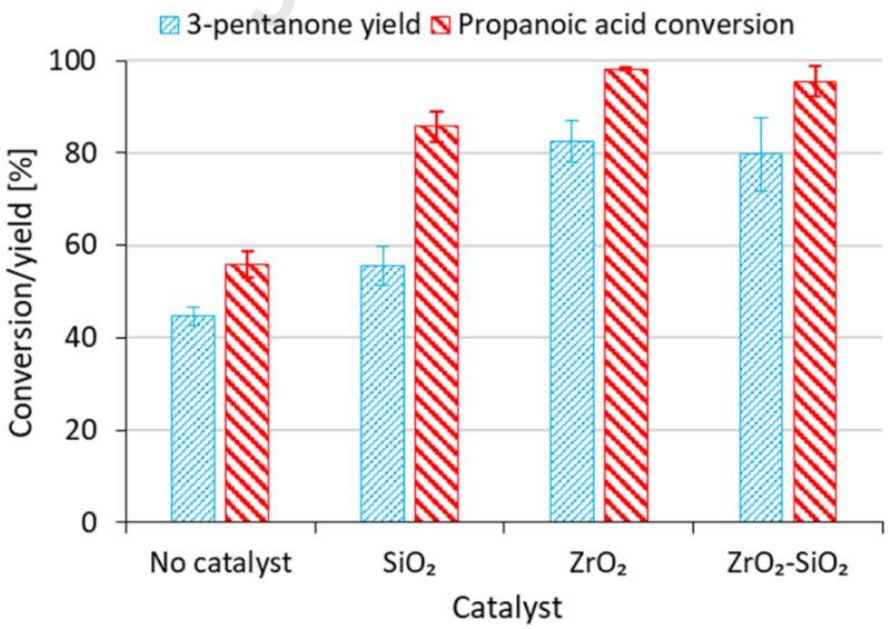

Figure 3. Conversion of propionic acid and yield of 3-pentanone for both non-catalytic and SiO_2, ZrO_2-SiO_2, and ZrO_2 catalysed ketonisation under 10 bar initial hydrogen pressure atmosphere, 350 °C reaction temperature, and 180 min reaction time.

The reducing effect of the hydrogen atmosphere is significant in both ZrO_2-SiO_2 and ZrO_2 catalysts. This is because the reactivity of surface oxygen due to ZrO_2 can be linked to the formation surface hydroxyl groups and oxygen vacancies [33], where part of the surface oxygen (coordinatively unsaturated O^{2-}) on ZrO_2 are reduced in the presence of hydrogen and water produced [34]. It suggests that during ketonisation of propionic acid, there is equilibrium between H_2, H_2O, surface hydroxyl groups, and oxygen vacancies on the ZrO_2 surface since water can also dissociate to produce OH groups on the catalyst surface. Thus, ZrO_2 could be exhibiting a redox catalyst characteristic with hydrogen atmosphere [33]. Thus, under hydrogen atmosphere the yields of 3-pentanone over highly amphoteric ZrO_2 (82.5%) and moderately amphoteric ZrO_2-SiO_2 (79.8%) were within the margin of experimental error unlike nitrogen atmosphere. Notably, most published works are on the vapour/gas phase ketonization of carboxylic acids on metal oxides catalysts using fixed-bed reactors; liquid phase batch systems have received little attention. Thus, the results of this study were compared with those reported in literature for the ketonisation of carboxylic acids in batch reactor systems. **Table 5** summarised how the results in literature compared with that obtained in the study. The conversion and yield achieved in this study are comparable to those found in the literature, according to the comparative analysis of the results (Table 5).

Table 5. Overview of ketonization of carboxylic acids in literature and this study

Catalyst	Conversion (%)	Yield (%)	Reference
ZrO_2		93.5	[39]
$CeZrO_2$		95.2	[39]
Red mud	100	41	[40]
Reduced red mud	94	61	[40]
$CeMO_x$ (M = Zr, Al, Fe, Mn)	89 - 90	44 - 87	[23]
ZrO_2/C	39	38	[41]
ZrO_2	98.1	82.5	This research result
ZrO_2-SiO_2	95.5	79.8	This research result

481 Consequently, the 3-pentanone produced by C-C coupling of the propionic acid via ketonisation
482 possesses a higher energy density due to its decreased oxygen content, which can be processed into
483 C_{10}–C_{15} ketones via aldol condensation, resulting in corresponding hydrocarbons following catalytic
484 hydrodeoxygenation for use as biofuels with a similar carbon number to petroleum-based fuels. The
485 presence of large molecular weight ketones than 3-pentanone such as 3-heptanone in the liquid
486 product suggests the slight occurrence of aldol condensation catalysed by ZrO_2 (**Tables S2** and **S3**).
487 However, study on the conversion of ketones produced from carboxylic acids ketonisation into longer
488 chain ketones via C-C coupling by aldol condensation has been reported elsewhere [42]. In a separate
489 piece of work, we reported aldol condensation of cyclohexanone (C_6), a model ketone C-C coupling
490 into C_{12}+ (dimeric 2-cyclohexylidenecyclohexanone and 2-(1-cyclohexen-l-yl) cyclohexanone), and
491 consequently carried out hydrodeoxygenation, which resulted in the production of aviation fuel-range
492 hydrocarbons (C_6-C_{16}) using $NbOPO_4$ catalyst. In the study, $NbOPO_4$ exhibited the highest catalytic
493 activity and selectivity (about 70% conversion and 66% selectivity) towards aldol condensate C-C
494 coupling adducts compared to Al_2O_3, SiO_2, ZrO_2 and ZrO_2-SiO_2 screened at 160 °C [42].

495

496 **3.2.1 Stability of ZrO_2 catalyst under nitrogen and hydrogen atmospheres**

497 The cost of the catalyst, which is critical to the overall economics of an industrial scale catalytic
498 process, is influenced by its stability, lifespan, and ability to be regenerated. The economic impact of
499 catalyst deactivation includes changes product composition, lower yield of desired product, and extra
500 cost incurred in the regeneration or replacement process. Therefore, the recovery and reuse of ZrO_2
501 catalyst would be highly desirable for a sustainable process. In terms of the catalyst stability, after
502 each experiment, the catalyst was recovered washed with acetone and dried at 105 °C for 6 h and
503 then reused for repeated experiment. At the end of the third cycle of repeated experiment, the
504 catalyst was regenerated via oxidation in air atmosphere at 500 °C for 2 hours. The result of an
505 additional test carried out to investigate the stability and reusability of ZrO_2 catalyst at 350 °C under

nitrogen and hydrogen atmosphere is shown in **Figure 4**. The chart shows that the yield of 3-pentanone decreased from 70% in the first use to 62% in the second cycle and remained at this level in the third cycle of ZrO_2 catalyst reusability, whereas the conversion of propionic acid is comparatively stable at roughly 90% for the three cycles under nitrogen atmosphere (Figure 4a). Whereas the ZrO_2 catalyst is relatively stable when the ketonisation of propionic acid carried out under hydrogen as indicated in the stability of conversion and yield within 95% and 73%, respectively (Figure 4b). ZrO_2 showed a significant deactivation resulting in the loss of activity in the first use before reaching steady state activity as can be observed in the second and third cycles (Figure 4a). This can be confirmed by the 8% decline in the yield of 3-pentanone between first and second cycles under nitrogen atmosphere, whereas only slight decrease of 4.9% occurred with hydrogen. Thus, after the first use, the ZrO_2 catalyst became relatively stable and resistance to further deactivation.

The slight loss of catalytic activity after the first can be attributed to a few factors carbon deposition, adsorption of 3-pentanone, and poisoning of CO_2. The results of the ZrO_2 catalyst stability and reusability test collaborate with its acidity and XRD pattern studies both before and after experiment (Section 3.2.2), which further confirm how propionic acid ketonisation desired product and byproducts affect catalytic activity. This is in line with the observed drop in acidity for the spent catalyst following ketonisation of propionic acid as compared to the fresh ZrO_2 catalyst, which is discussed in Section 3.2.2.

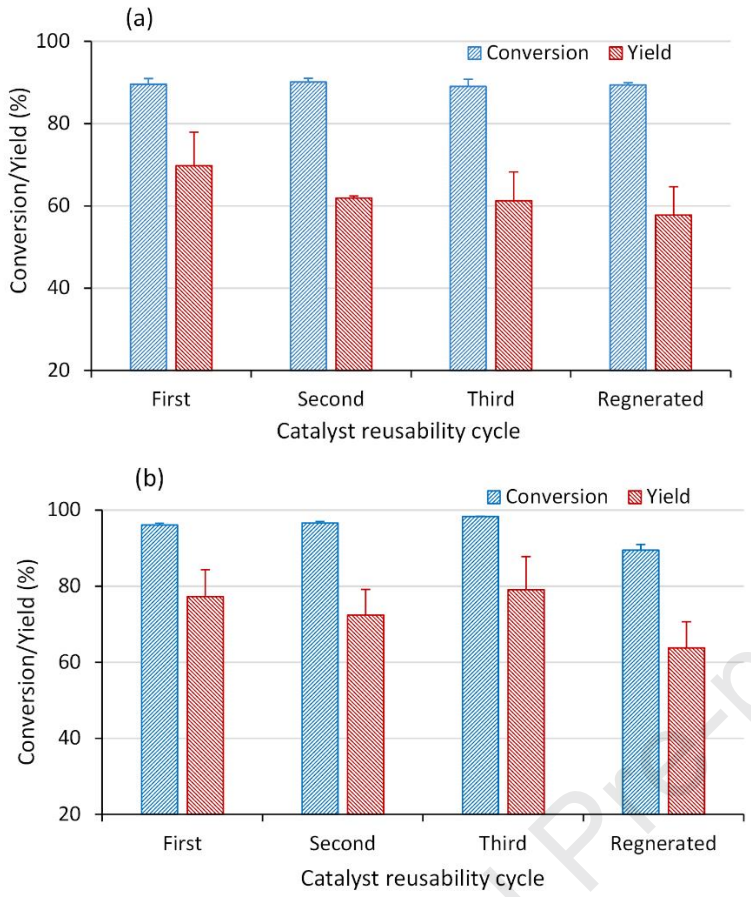

Figure 4. Stability and reusability of ZrO_2 catalyst for ketonisation of propionic acid at 350 °C temperature, 180 min reaction time, and 10 bar initial pressure: (a) nitrogen atmosphere and (b) hydrogen atmosphere.

The adsorption of propionic acid itself [1], the C-C coupling condensation product (i.e., 3-pentanone and other ketones) on the active sites of the ZrO_2 (amphoteric solid) catalyst [43], and coke formation [44], could be responsible for the profound deactivation observed in the first use. Consequently, the spent ZrO_2 catalyst was notably dark compared with the fresh ZrO_2, which can be attributed to coke deposition on the catalyst. This implies that under hydrogen atmosphere the formation carbon during the ketonisation of propionic acid is reduced relative to nitrogen. This is consistent with the observation of solid yields reported in **Table 1** for 350 °C, 10 bar, and 180 min, which shows that the carbon yield is greater under nitrogen atmosphere than hydrogen. However, the regenerated ZrO_2 catalyst though exhibited a similar conversion for propionic acid but the yield of 3-pentanone is about 12% lower than that achieved on first use under nitrogen atmosphere. Nonetheless, the results shown

in Section 3.2.2 demonstrated that the specific surface area, pore volume, and acid-base strength could be restored through oxidative regeneration of the spent ZrO_2 catalyst. Even though oxidative regeneration would have burn-off deposited carbon and adsorbed pentanone on the active sites, the activity of the regenerated ZrO_2 catalyst is only comparable to the second and third cycles in terms of 3-pentanone yield (**Figure 4a**). It has been reported that the significant amount of CO_2 produced as a reaction by-product during propionic acid ketonisation can potentially poison the basic sites of basic and amphoteric solid oxides catalysts [44], [45]. Based on this result, it is evident that two issues that require adequate consideration further research towards industrial scale ketonisation are catalyst stability and active site regeneration.

Based on the deposited solid char on the spent catalysts observed in **Tables 2** and **4** at 350 C and 180 min, indicate that deactivation of the ZrO_2 catalyst could therefore be predominantly credited to the catalyst coking. The GC/MS products (**Tables S2** and **S3**) and gas composition in **Table 3** show that in the presence of hydrogen decarboxylation and decarbonylation result in the formation of light gasses (CO_2 or CO) and mostly alkanes, as illustrated in **Reaction Scheme 1**. It has been reported that during carboxylic acid ketonisation reaction, catalyst base sites are poisoned by adsorbed CO_2 by-product [44], [46]. So, the higher concentration of CO_2 in the produced gas under nitrogen than hydrogen could have contributed to the significant deactivation of catalyst observed in **Figure 4**.

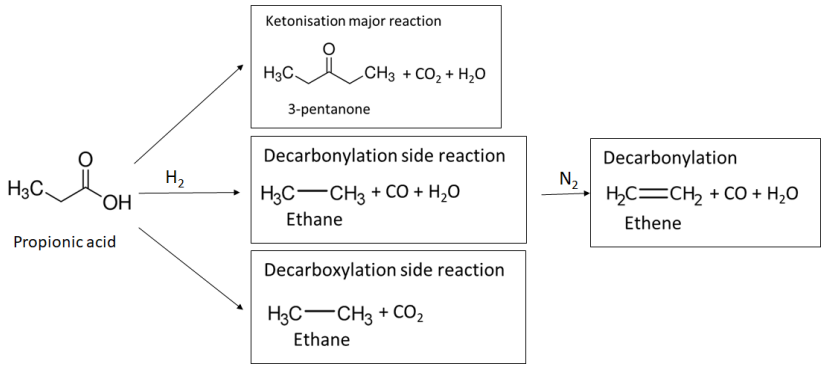

Reaction Scheme 1. Generic reaction network and the role of hydrogen.

Furthermore, the presence of hydrogen gas in produced gas in **Table 3** under nitrogen atmosphere indicates the occurrence of dehydrogenation, which results in the formation of ethene in decarbonylation of propionic acid (**Reaction Scheme 1**). Mechanistically, the C–H bonds in C_1-C_4 are broken by proton abstraction at the Lewis acid sites on the catalyst surface, with constant abstraction of hydrogen triggering coke formation precursors [47]. Moreover, secondary and tertiary self-/cross-aldol condensation of the produced 3-pentanone (**Tables S2** and **S3**), followed by oligomerisation on the acid sites in the catalyst pores at relatively high temperatures, have been suggested as another plausible route to coke formation in the ketonisation of propionic acid [48]. Therefore, olefinic reaction intermediates are potential coke precursors. In addition to C–C cleavage, olefin oligomerisation, and deep dehydrogenation under nitrogen atmosphere promoted coke formation leading to higher catalyst deactivation (**Figure 4**). This can also be confirmed in **Tables 2** and **4**, showing decreased char yield from 2.2 wt% (nitrogen atmosphere) to 0.9 wt% (hydrogen atmosphere). Therefore, olefins formation and hydrogen abstractions from C_1-C_4 are greatly suppressed under hydrogen atmosphere.

3.2.2 Catalysts characterisation

The XRD patterns of the synthesised single metal oxides (weak acid SiO_2 and highly amphoteric ZrO_2), and moderately amphoteric mixed metal oxides of SiO_2-ZrO_2 catalysts can be found in the **supplementary information Figure S2**. A large peak can be seen at 2θ equals 22.5° for the synthesised SiO_2 and ZrO_2-SiO_2 catalyst materials XRD patterns, indicating that their grain size is nano-sized and amorphous in nature (**Figure S2**). However, to gain insight into the effect of propionic acid ketonisation product, reactant, and byproducts on the catalyst structure and catalytic performance at 350 °C reaction temperature and 180 min time, the synthesised ZrO_2 catalyst XRD pattern before reaction, postreaction, and regenerated were compared. The XRD patterns of the synthesised fresh, spent, and regenerated ZrO_2 catalysts are shown in **Figure 5**. The postreaction catalyst characterisation shows

585 several changes relative to the fresh ZrO_2 material. The catalyst XRD pattern of synthesised ZrO_2
586 exhibited high crystallinity with notable peaks corresponding to monoclinic and tetragonal phases of
587 the material (**Figures 5a and 5b**). The crystalline structure, identified peaks, and phases are consistent
588 with that reported in the literature for ZrO_2 [49], [50]. The monoclinic crystalline phases can be
589 identified at 2θ = 24.3° (110), 28.3° (11$\bar{1}$), 31.5° (111), 40.6° (102), 45.2° (211), 65.8° (231), and 75°
590 (041), while the tetragonal crystal phases are at 2θ = 30.3° (011), 35° (110), 50.2° (112), and 60° (121)
591 [50], [51]. This collaborates with ZrO_2 synthesised by precipitation method [50].

592

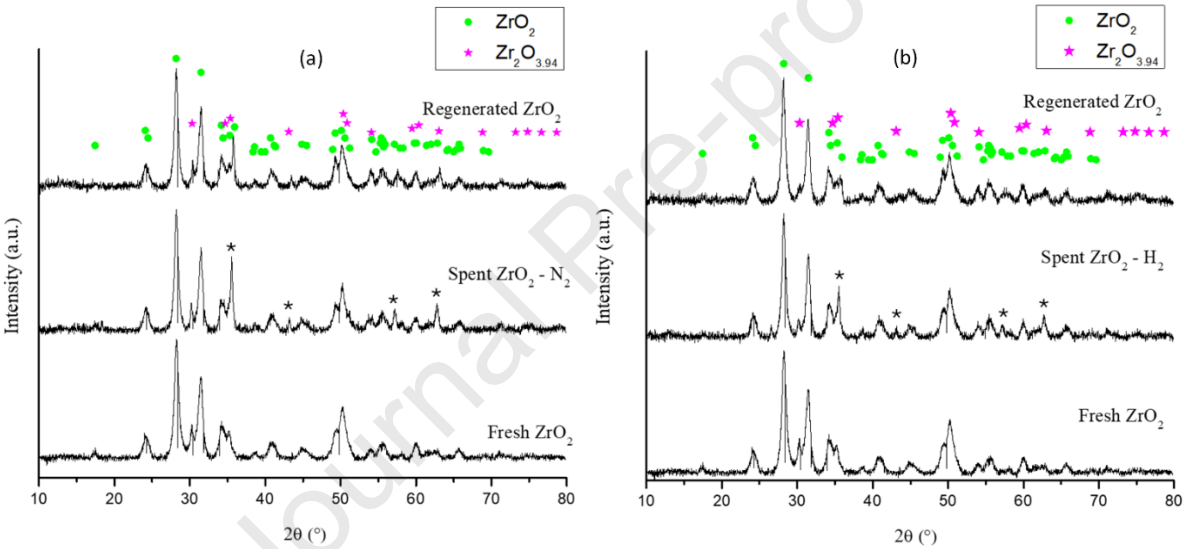

593
594 **Figure 5**. XRD patterns: (b) fresh, spent and regenerated ZrO_2 after ketonisation in N_2 atmosphere, (b)
595 XRD profiles of fresh, spent and regenerated ZrO_2 after ketonisation in H_2 atmosphere.

596

597 The structural changes in the oxide phase can be attributed to a reaction of the propionic acid with
598 the zirconia [12], resulting in the formation of metal carboxylate [23]. After propionic acid is ketonised,
599 the XRD profile of the spent ZrO_2 shows four extra peaks, but the intensity of these peaks is higher for
600 ketonisation in a nitrogen atmosphere than in a hydrogen atmosphere. The presence of four
601 additional peaks in the XRD patterns of spent ZrO_2 catalyst indicate impurity phase(s) due to the
602 adsorption of propionic acid, 3-pentanone, and carbon deposition. Whereas a compositional phase
603 change can be observed in the regenerated catalyst (**Figures 5a and 5b**). These observed changes in
604 the postreaction spent ZrO_2 catalyst relative to its fresh is consistent with XRD profiles reported for

postreaction of rare earth oxides (La_2O_3, CeO_2, Pr_6O_{11}, and Nd_2O_3) after acetic acid ketonisation at 350 °C [12]. This explains the decline in ZrO_2 catalyst activity and selectivity towards 3-pentanone shown in **Figure 4**. Consequently, the impurities and structural phase changes observed in the regenerated ZrO_2 in **Figure 5**, is the reason for the decreased catalytic performance in terms of conversions and yields observed in **Figure 4**.

The nitrogen adsorption-desorption isotherm of ZrO_2 catalyst and its pore size distribution before reaction, postreaction, and regenerated is displayed in **Figure 6**. The Brunauer–Emmett–Teller (BET) equation was used to estimate the specific surface areas using the nitrogen adsorption isotherm data. Whereas the pore sizes and pore volumes were calculated using the Barrett, Joyner, and Halenda's (BJH) method based on the isotherm desorption branch and multipoint approach. The obtained isotherm was found to be Type IV, indicating a mesoporous material with weak adsorbent–adsorbate interactions. The H3-type hysteresis loops reflected pores including plate slit structure, crack, and wedge (**Figure 6a**). **Table 6** shows the synthesised catalysts specific surface areas, pore sizes, and pore volumes. The pore diameter of the catalyst fell within the mesopore range of 2-50 nm (**Figure 6b**). The mesoporous structure, specific surface and pore size obtained in this study are within the range reported in the literature for ZrO_2 material [51].

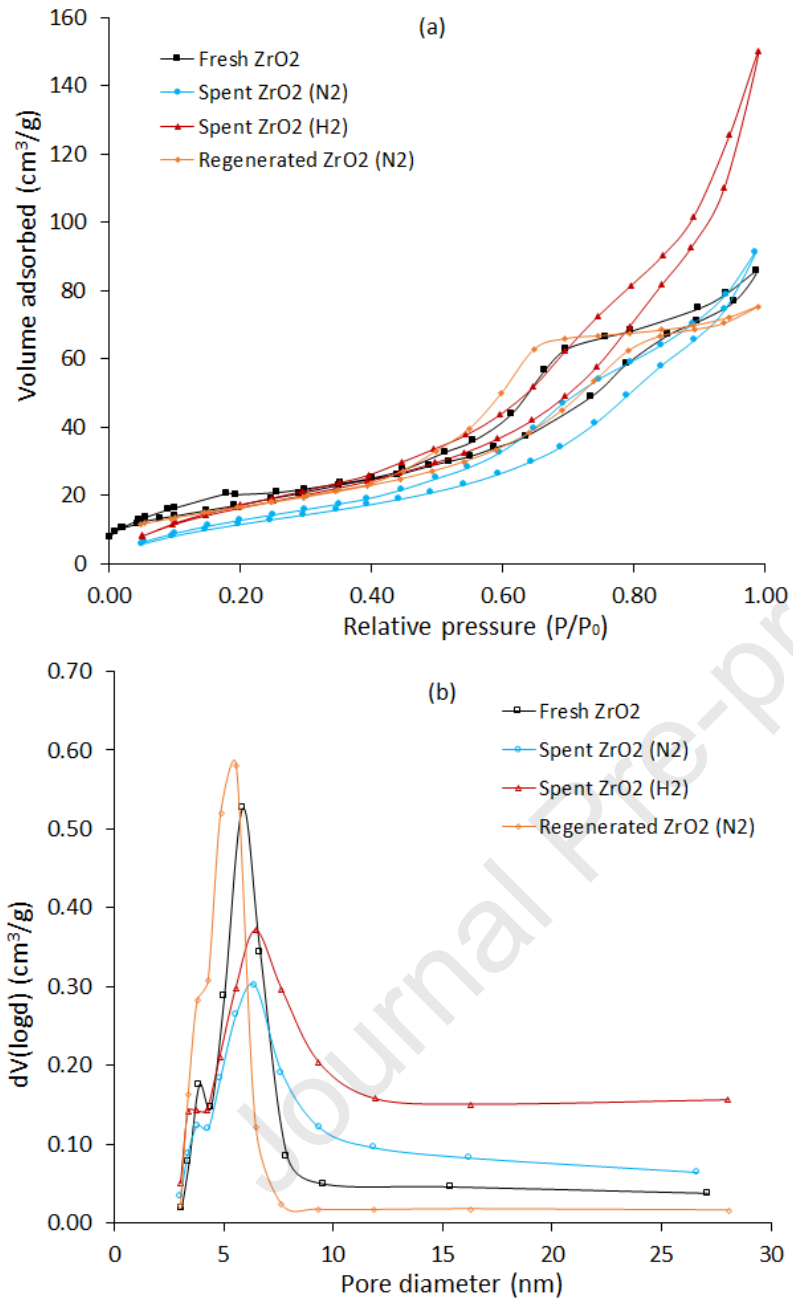

Figure 6. Nitrogen physisorption: (a) nitrogen adsorption-desorption isotherm of fresh, spent and regenerated ZrO_2, and (b) pore size distribution of fresh, spent and regenerated ZrO_2.

Table 6. Textural properties of the synthesised fresh catalysts (ZrO_2, SiO_2-ZrO_2, and SiO_2) as well as spent and regenerated ZrO_2 catalyst.

Catalyst	**Specific surface Area [m²/g]**	**Pore Volume [cm³/g]**	**Pore Diameter [nm]**
Fresh SiO_2	196.9	0.42	5.0
Fresh ZrO_2 - SiO_2	224.1	0.62	9.9

Fresh ZrO_2	61.9	0.13	5.9
Spent ZrO_2 (N_2)	49.8	0.13	5.6
Regenerated ZrO_2 (N_2)	62.7	0.13	2.4
Spent ZrO_2 (H_2)	70.5	0.21	6.5
Regenerated ZrO_2 (H_2)	115.3	0.11	3.6

The textural differences in fresh, spent, and regenerated catalysts, as can be observed in the nitrogen physisorption isotherm, indicate structural alterations caused by propionic acid ketonisation (**Figures 6a and 6b**). It can be observed that doping ZrO_2 with SiO_2 increased the mixed oxide SiO_2-ZrO_2 specific surface area of the catalyst relative ZrO_2 catalyst (**Table 6**). This is consistent with the literature [25]. The specific surface areas and pore volumes of the prepared catalysts increased in the order ZrO_2-SiO_2 >> SiO_2 >> ZrO_2. However, despite the specific surface area of the catalysts increasing in the order SiO_2–ZrO_2 > SiO_2 > ZrO_2, the conversions of propionic acid and the yields of 3-pentanone follow the order ZrO_2 > SiO_2–ZrO_2 > SiO_2 (**Figures 1** and **3**). This implies that ketonisation of propionic acid is mostly dependent on the amphoteric nature of the catalyst than its specific surface area. The pore diameters of the catalysts fell within the mesopore range of 2-50 nm (**Supplementary information Figure S3**), whereas the pore size of ZrO_2-SiO_2 two times that of SiO_2 (**Table 6**). The specific surface area of the spent ZrO_2 catalyst decreased significantly from 61.85 m^2/g to 49.83 m^2/g, which is 19.4% drop after ketonisation in nitrogen atmosphere (**Table 6**). The plausible reasons for the specific surface area lost are the deposition of carbon, product and byproducts adsorption, and reaction-induced pore restructuring. The catalyst pore size region of 5–6 nm is slightly plugged for the spent ZrO_2, suggesting that most of the ketonisation reaction takes place there (Figure 1d). However, the specific surface area and pore volume of both the regenerated and fresh ZrO_2 are comparable, suggesting that oxidative regeneration of spent catalyst could restore catalytic activity. On the other hand, a 14% increase in specific surface area of the spent ZrO_2 from 61.85 m^2/g to 70.54 m^2/g was observed after propionic acid ketonisation in a hydrogen atmosphere. This is due to reaction-induced pore size

broadening [23]. This is evident in the pore size distribution results shown in **Figure 6b**, where the pore size ranges are as follows: 3 – 9.5 nm (fresh ZrO_2), 3 – 11.8 nm (spent ZrO_2 under N_2), and 3 – 12 nm (spent ZrO_2 under H_2).

It has been reported that the catalytic activity of ZrO_2 catalyst for ketonisation of carboxylic acids correlates linearly with the total densities of the acidic and basic sites [51]. The IR spectra from the pyridine-FTIR due to the adsorption of pyridine onto the fresh catalysts (ZrO_2, SiO_2-ZrO_2, and SiO_2) as well as spent and regenerated ZrO_2 catalysts are shown in **Figure 7**. The vertical lines on the chart designate the vibration bands characteristic for pyridine adsorbed onto the ZrO_2 catalyst acid sites. The bands occur at 1444 cm^{-1}, 1490 cm^{-1}, and 1540 cm^{-1} due to adsorbed pyridinium ion and pyridine. These three acid sites are indicative of the presence of the Lewis, Brønsted and both acid sites. The band at wavenumber 1444 cm^{-1} denotes the Lewis acid site because of the acid-base $Zr^{4+}O^{2-}$ pair, the band at 1490 cm^{-1} which is moderate acid (combined Lewis and Brønsted acid sites), and at 1540 cm^{-1} is the strong Brønsted acid site due to the -OH group on ZrO_2 [32], [52]. The strengths of the acid site types are presented in **Table 7**. The Lewis plus Brønsted acid sites strength follow identical pattern to the conversion and yields reported in **Figures 1** and **3** (ZrO_2 > SiO_2-ZrO_2 > SiO_2). Doping ZrO_2 with equal amount of SiO_2, increased the Lewis acid site strength and decreased the Brønsted acid site in the binary oxide SiO_2-ZrO_2 relative to pure SiO_2 and ZrO_2 (**Table 6**). This collaborates with literature that the density of the basic sites decreased with the doping of ZrO_2 with SiO_2 (an acidic oxide) to form binary oxide of SiO_2-ZrO_2 [25]. Thus, the performance of the catalysts in terms of conversions and yields can be linked the amphoteric nature of the single and binary oxides. This is consistent with the order of ketonisation activities observed from the catalysts in **Figures 1** and **3**, which follows strong amphoteric oxide (ZrO_2), moderate amphoteric binary oxide (SiO_2-ZrO_2), and acidic oxide (SiO_2).

It can be observed that the synthesised ZrO_2 catalyst shows equal strength Lewis and Brønsted acid sites strength. The changes in the strengths of the Lewis, Brønsted, and Lewis plus Brønsted acid sites for the fresh, spent, and regenerated ZrO_2 affirm that these active sites are responsible for the

catalytic activity and its ketonisation performance. It has been reported that during ketonisation of carboxylic acids that the Lewis acid sites are known to induce carboxylate stabilisation and activation of the second carboxylic acid [7], while Brønsted sites are required for α-H abstraction and carboxylic acid coordination [53].

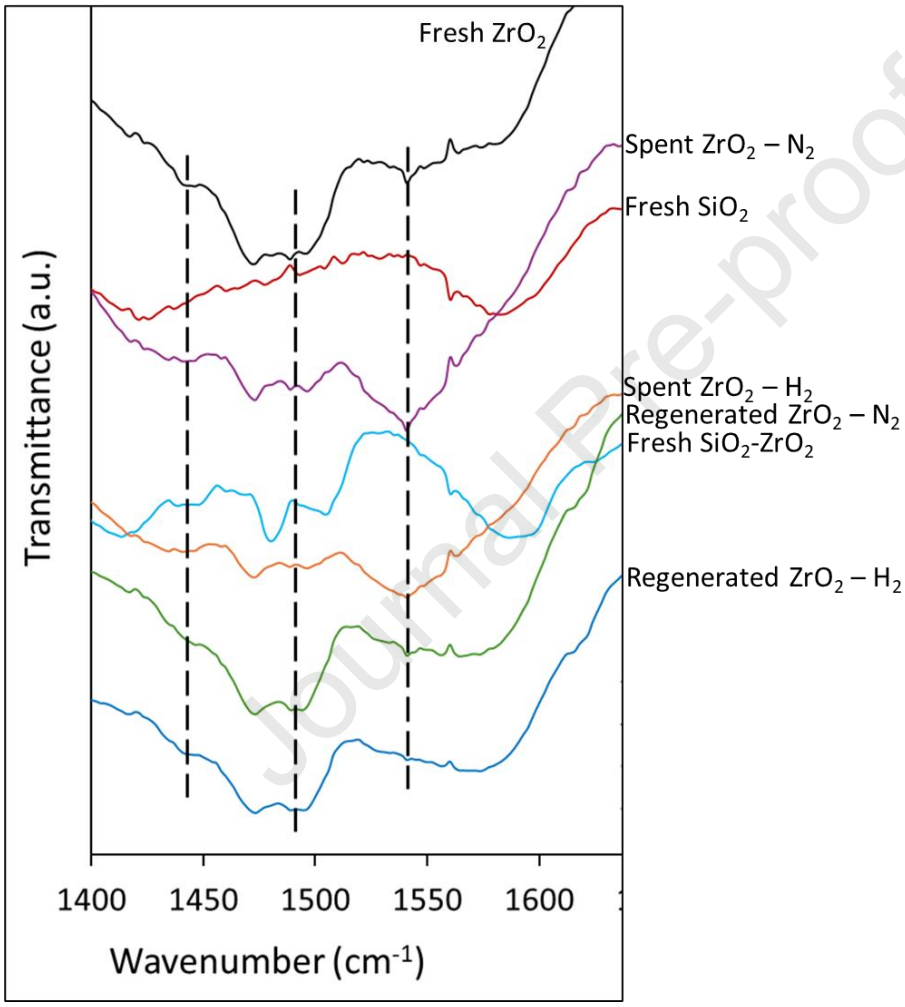

Figure 7. Pyridine-FTIR spectra profiles of fresh catalysts (ZrO_2, SiO_2-ZrO_2, and SiO_2), spent, and regenerated ZrO_2 catalyst after ketonisation under hydrogen and nitrogen atmospheres.

688 **Table 7**. Acid site types and strength for fresh catalysts (ZrO_2, SiO_2-ZrO_2, and SiO_2) as well as spent
689 and regenerated ZrO_2 catalyst after ketonisation under hydrogen and nitrogen atmospheres at 350
690 °C and 180 min.

Catalyst	Lewis (mmol g^{-1})	Brønsted (mmol g^{-1})	Lewis + Brønsted (mmol g^{-1})
SiO_2	0.66	9.50	10.70
SiO_2-ZrO_2	12.14	4.67	16.00
Fresh ZrO_2	8.11	8.11	16.38
Spent ZrO_2 - H_2	1.79	3.16	5.47
Spent ZrO_2 - N_2	2.50	12.84	15.64
Regenerated ZrO_2 - H_2	7.15	2.83	9.91
Regenerated ZrO2 - N_2	7.28	5.10	14.40

691

692 The strength of the ZrO_2 catalyst Lewis's acid site decreased from 8.11 mmol g^{-1} to 1.79 mmol g^{-1} (spent
693 catalyst after ketonisation under hydrogen atmosphere) and to 2.50 mmol g^{-1} (spent catalyst after
694 ketonisation under hydrogen atmosphere), representing 78% and 69% drop, respectively. While the
695 Brønsted acid site dropped by 61% for spent catalyst after ketonisation in hydrogen atmosphere and
696 65% (regenerated). The adsorbed 3-pentanone produced during the ketonisation of propionic acid,
697 byproducts, and deposited coke were thought to be the cause of the decrease in the strength of acid
698 sites on the spent catalyst [43], [44]. These changes in the strength of the amphoteric nature ZrO_2 due
699 to adsorption of molecules explain the declining trend in activity and selectivity with reusability
700 towards the yield of 3-pentanone especially under nitrogen atmosphere as can be observed in **Figure**
701 **4**. Notably, the oxidative regeneration of the spent catalyst significantly restored the strength of the
702 Lewis acid site compared to the Brønsted acid site. This suggested that the main product and side
703 products strongly adsorbed onto the Brønsted acid site such that 500 °C regeneration temperature
704 was not fully effective. However, oxidative regeneration at 500 °C can significantly restore the overall
705 acidity of spent ZrO_2 catalyst. Consequently, these results suggested that the Lewis acid site was
706 mainly responsible for the propionic acid ketonisation compared to the Brønsted acid sites of ZrO_2.

707 When the ketonisation reaction was carried out in a nitrogen atmosphere, the strength of the
708 Brønsted acid site of the spent catalyst increased, which implied that propionic acid was strongly
709 adsorbed onto the ZrO_2 catalyst. The decrease in Brønsted acid site strength after oxidative

regeneration of the spent ZrO_2 catalyst following ketonisation in a nitrogen and hydrogen atmosphere helped in confirming this hypothesis (Table 2). Similarly, strong adsorption of propionic acid on monoclinic phase of ZrO_2 around the same band range has been reported in the literature [35], [54]. Thus, the propionic acid adsorbs on the ZrO_2 catalyst surface molecularly or dissociatively, resulting in monodentate or bidentate carboxylates [53]. Therefore, the reduction in the strength of acid sites strength due to adsorption of propionic and 3-pentanone after ketonisation as shown in Table 7, explains the trend in terms of conversion and yield of 3-pentanone observed in **Figure 4**.

3.3 Preliminary study on the effect of bio-oil compounds on propionic acid ketonisation

The effect of bio-oil compounds on the ketonisation of propionic acid was studied at the optimum reaction temperature, time and atmosphere (H_2) using propionic acid/bio-oil ratio of 1:1 (g/g) and ZrO_2 catalyst. **Table 8** shows the impact of bio-oil compounds on products distribution, propionic acid conversion, and 3-pentanone yield. The results show that the presence of bio-oil significantly increased the char (i.e., solid) and gas yields at the expense of liquid compared to the propionic acid feedstock alone. The high gas formation in the presence of bio-oil can be attributed to the short-chain (C_1-C_4) organic compounds (***see Supplementary Information Table S4***). Hence, thermally unstable compounds in bio-oil (e.g., sugars, ethers) [20], readily undergo deoxygenation via decarboxylation and decarbonylation into light hydrocarbons gas. Whereas the increased char formation is due to polymerisation and condensation of char-forming intermediates (e.g., polyaromatics) [55], at the acidic/basic sites of the ZrO_2. Additionally, ZrO_2 catalysed bio-oil upgrading affirms high char and gas formation (**Table 8**).

Table 8. Effect of bio-oil on propionic acid conversion, products distribution, and 3-Pentanone yield (7.5 g bio-oil, 7.5 g propionic acid, 1 g ZrO_2, 10 initial H_2 pressure, 350 °C temperature after 180 min).

Products yields	**Propionic acid**	**Propionic acid+Bio-oil**	**Bio-oil**
Solid (wt%)	1.00±0.133	6.52±0.15	14.42±2.04
Liquid (wt%)	58.33±5.93	43.14±1.72	38.43±2.52
Gas (wt%)	36.07±5.33	50.30±2.18	45.58±3.28
Mass balance (wt%)	95.40±4.24	99.96±0.03	98.44±1.03
Conversion (%)	98.1±0.26	95.73±0.45	
3-Pentanone yield (wt%)	82.5±2.18	33±3.41	

732 Notwithstanding, a propionic acid conversion of 95.73% obtained in the presence of 50 wt% bio-oil is
733 comparable to that achieved when ketonisation of pure propionic acid was carried out (**Table 8**).
734 However, the yield of 3-pentanone significantly decreased due to the presence of bio-oil relative to
735 pure propionic acid. This could be due to a number of reasons: (1) the organic compounds in the bio-
736 oil and propionic acid competed for the active sites of the ZrO_2 catalyst, (2) the formation of char could
737 have covered the active sites on the catalyst surface, thereby activating undesirable side reactions,
738 and (3) activation of other competing reactions such as cross-ketonisation with other carboxylic acids
739 in the bio-oil, alkylation, and C-C cleavage of formed ketones.

740 After reviewing the formed compounds from the GC/MS analysis results (***see Supplementary***
741 ***Information Tables S5 and S6***), the increased contents of ketones in the liquid product of propionic
742 acid+bio-oil feedstock indicate that the propionic acid participated in forming other ketonisation
743 products via cross coupling with other carboxylic acids or compounds that could be hydrolysed to
744 carboxylic acids (e.g., esters). However, comparing the compounds in liquid products from propionic
745 acid only, propionic acid+bio-oil, and bio-oil only (**Tables S2**, **S5**, and **S6**), it is clear that the ZrO_2 catalyst
746 was very selective towards ketonisation and enhanced cross ketonisation of propionic acid and other
747 acids in the bio-oil. Notably, most of the carboxylic acids either in the bio-oil or formed during the
748 reaction are ketonised by the ZrO_2 catalyst (**Tables S2**, **S5**, and **S6**). This can be confirmed by the
749 abundant and the wide range of ketones in the liquid product from propionic acid+bio-oil feedstock,
750 with major ones ranked as follows: 3-pentanone > 2-butanone > 3-hexanone > 2-methyl-3-pentanone
751 > 2-pentanone > 4-methyl-3-hexanone and other longer chain ketones (***see Supplementary***
752 ***Information Table S5***). Based on the range of ketonic compounds formed, it can be deduced that
753 propionic acid undergone both self-ketonisation into 3-pentanone which is the desired product, cross-
754 ketonisation into C_6-C_{20} straight and branched chain ketones, C-C cleavage into short-chain ketones
755 (e.g., 2-butanone), alkylation (e.g., 2-methyl-3-pentanone), and isomerisation (e.g., 3-pentanone/2-
756 pentanone), respectively. The other compounds are mostly hydrocarbons formed by dehydration of
757 ketones, decarbonylation, and decarboxylation (**Table S5** and **S6**). These reactions are dominant in the

presence of bio-oil than pure propionic acid ketonisation. Hence, these additional reactions significantly affected the yield of 3-pentanone in the final liquid product. These ketonic compounds obtained in this work can serve as feedstock for aldol condensation into longer-chain ketones which fall within aviation fuel range precursors. Therefore, to produce aviation fuel range hydrocarbons, the next steps will involve investigating the subsequent studies that will facilitate the integration of sequential ketonisation, aldol condensation, and hydrodeoxygenation based on experimental results.

4. Future perspective

The optimal catalyst can be tuned and modified for more realistic feedstocks following this simplified model compound approach study carried out using batch reactor, which enables catalyst screening, development, and performance evaluation. Hence, this study has provided further insight into the significant role played by the amphoteric property of ZrO_2 catalyst in ketonisation of carboxylic acids. However, working with actual propionic acid derived from bio-oils are significantly more complex due to presence of other components. Further research should therefore investigate the performance of ZrO_2 and other highly amphoteric oxide catalysts in terms of the conversion of propionic acid and the yield of 3-pentanone in the presence of other bio-oil components. This would allow understanding of the interactions between different molecules due to the presence of other bio-oil components and how their competition for the acidic-basic sites of the catalyst may impact the ketonisation reaction. As a result, the results can closely mimic real bio-oil upgrading. In our previous study, the effect of bio-oil addition on to a “clean” ketone feedstock solvent-free self-aldol condensation was investigated [42]. It was found that the presence of the bio-oil increased formation of solid residue and suppressed gas formation. Additionally, the conversion and selectivity significantly decreased as the organic compounds in the bio-oil competed with the ketone for the catalyst's acid sites.

Consequently, this study confirms that catalysts will play a pivotal role in both the process economics and scale up. Additionally, one of the challenges to the commercialisation of catalytic ketonisation of

783 carboxylic acids is catalyst deactivation [44]. This implies that research into the development of robust,
784 low-cost, high amphoteric, selective, and stable catalysts would contribute towards application in the
785 ketonisation of carboxylic acids found in real bio-oil, process scale up, and commercialisation.
786 Therefore, it would be advantageous to conduct further investigation into the reaction mechanism
787 using a batch reactor for kinetic modelling development. Additionally, investigations on continuous
788 flow reactors are pertinent for the transition to industrial applications. Another aspect of interest is a
789 study on the sequential ketonisation of propionic acid followed by aldol condensation of the 3-
790 pentanone, and then, catalytic hydrodeoxygenation into corresponding hydrocarbons biofuel. In
791 comparison to fossil-based propionic acid, biomass-derived propionic acid leads to around 60%
792 reduction in greenhouse gas emissions requiring about twofold primary energy input for production
793 [17]. It can be deduced that the transition from biomass to biofuel conversion technologies are energy
794 intensive on industrial scale. Thus, biomass-derived propionic acid for 3-pentanone and sustainable
795 biofuel production technologies need to be able to economically compete with petroleum-based
796 analogues on an industrial scale to be successful. Therefore, future investigation will include the
797 supply chain of biomass-derived short-chain carboxylic acids, their ketonisation, further C-C coupling
798 of resulting ketones to make longer-chain liquid hydrocarbon fuel precursors and their eventual
799 hydrodeoxygenation to fuel-range liquid hydrocarbons by developing process models based on mass
800 and energy balances to evaluate environmental sustainability and process economics.

801 **Conclusion**

802 This study has evaluated the ketonisation of propionic acid over synthesised metal oxide catalysts with
803 different surface acidity/basicity properties, including mesoporous ZrO_2, SiO_2 and SiO_2-ZrO_2over a
804 temperature range 300 °C to 400 °C and nitrogen/hydrogen atmospheres to produce 3-pentanone.
805 The ZrO_2 catalyst gave the best catalytic activity and selectivity of propionic acid ketonisation towards
806 3-pentanone. Results indicate that the amphoteric nature of ZrO_2 influenced its catalytic performance
807 compared to the performance of the slightly acidic SiO_2 and the SiO_2-dope ZrO_2 with changed surface

properties. Compared to the other two catalysts, possibly large surface oxygen vacancies on ZrO_2, helped to reduce formation of stable intermediates that could form other competing products. This is due to the acid–base bifunctional property of ZrO_2 attributed to the amphoteric (Brønsted basic or acidic) hydroxyl groups of zirconia, and the Lewis basic sites comprising of co-ordinately unsaturated O^{2-} species and the Lewis acidic sites of Zr^{4+} species enhanced its ketonisation activity and selectivity towards ketone formation. The performance of the ZrO_2 catalyst was further enhanced under hydrogen atmosphere, leading to increased conversion, lower char formation and increased yield of the target 3-pentanone in the liquid product. Reaction conditions of 350 °C and reaction time of 180 minutes were optimal for the conversion of propionic acid and yield of 3-pentanone. Consequently, the ZrO_2 catalyst exhibited excellent ketonisation activity catalysing self-ketonisation of propionic acid and cross-ketonisation with other carboxylic acids found in bio-oil for a reaction involving 1:1 mass ratio mixture of propionic acid and a sample of pyrolysis bio-oil. In this work, ketonisation under hydrogen atmosphere appeared to have improved the stability of the ZrO_2 catalyst by converting intermediate species and preventing their deactivating effect via coke formation on the catalyst surface. Future work will explore the combination of relevant chemistries (e.g., ketonisation, aldol condensation and hydrodeoxygenation of oxygenated C-C coupled adducts) to convert short-chain carboxylic acids to produce liquid range hydrocarbons. Results from such studies will enable to development of process models for evaluating the scalability, environmental sustainability and economic viability of the combined process.

Funding

This work was supported by Innovate UK Energy Catalyst Round 8: Clean Energy - Experimental Development (Project Number 75521) and Innovate UK Energy Catalyst Round 9 – Mid Stage (Project Number 10047783).

CRediT authorship contribution statement

Abarasi Hart: methodology, data analysis and data curation, writing – original draft, writing – review & editing; **Himanshu Patel**: methodology, acquisition of data, analysis and interpretation of data; **Eyup Yildirir**: methodology, acquisition of data, analysis and interpretation of data; **Jude A. Onwudili**: conception and design of the study, project administration, resources, supervision, writing – original draft, writing – review & editing, final approval of submitted version.

Acknowledgements

The authors would like to thank the Innovate UK for funding this work. In addition, the authors are grateful to the Energy & Bioproducts Research Institute (EBRI) and Aston University, UK for all the support received.

Data Availability Statement

All relevant data generated from this work have been included in this Manuscript and Supplementary Materials. Authors are happy to consider any request for additional data.

862 **Reference**

863 [1] B. Boekaerts and B. F. Sels, "Catalytic advancements in carboxylic acid ketonization and its
864 perspectives on biomass valorisation," *Appl Catal B*, vol. 283, p. 119607, Apr. 2021, doi:
865 10.1016/j.apcatb.2020.119607.

866 [2] J. A. Onwudili and C. A. Scaldaferri, "Catalytic upgrading of intermediate pyrolysis bio-oil to
867 hydrocarbon-rich liquid biofuel via a novel two-stage solvent-assisted process," *Fuel*, vol. 352,
868 p. 129015, Nov. 2023, doi: 10.1016/j.fuel.2023.129015.

869 [3] P. Li *et al.*, "Bio-oil from biomass fast pyrolysis: Yields, related properties and energy
870 consumption analysis of the pyrolysis system," *J Clean Prod*, vol. 328, p. 129613, Dec. 2021,
871 doi: 10.1016/j.jclepro.2021.129613.

872 [4] R. Venderbosch and H. Heeres, "Pyrolysis Oil Stabilisation by Catalytic Hydrotreatment," in
873 *Biofuel's Engineering Process Technology*, 2011, p. http://dx.doi.org/10.5772/18446. [Online].
874 Available: www.intechopen.com

875 [5] A. Demirbas, "The influence of temperature on the yields of compounds existing in bio-oils
876 obtained from biomass samples via pyrolysis," *Fuel Processing Technology*, vol. 88, no. 6, pp.
877 591–597, Jun. 2007, doi: 10.1016/j.fuproc.2007.01.010.

878 [6] L. Fan *et al.*, "Bio-oil from fast pyrolysis of lignin: Effects of process and upgrading
879 parameters," *Bioresour Technol*, vol. 241, pp. 1118–1126, 2017, doi:
880 10.1016/j.biortech.2017.05.129.

881 [7] T. N. Pham, T. Sooknoi, S. P. Crossley, and D. E. Resasco, "Ketonization of carboxylic acids:
882 Mechanisms, catalysts, and implications for biomass conversion," *ACS Catal*, vol. 3, no. 11,
883 pp. 2456–2473, Nov. 2013, doi: 10.1021/cs400501h.

884 [8] G. Pacchioni, "Ketonization of carboxylic acids in biomass conversion over TiO2 and ZrO2
885 surfaces: A DFT perspective," Sep. 05, 2014, *American Chemical Society*. doi:
886 10.1021/cs500791w.

887 [9] E. I. Gürbüz, E. L. Kunkes, and J. A. Dumesic, "Integration of C-C coupling reactions of
888 biomass-derived oxygenates to fuel-grade compounds," *Appl Catal B*, vol. 94, no. 1–2, pp.
889 134–141, Feb. 2010, doi: 10.1016/j.apcatb.2009.11.001.

890 [10] O. Nagashima, S. Sato, R. Takahashi, and T. Sodesawa, "Ketonization of carboxylic acids over
891 CeO 2-based composite oxides," *J Mol Catal A Chem*, vol. 227, no. 1–2, pp. 231–239, Mar.
892 2005, doi: 10.1016/j.molcata.2004.10.042.

893 [11] M. Gliński, G. Zalewski, E. Burno, and A. Jerzak, "Catalytic ketonization over metal oxide
894 catalysts. XIII. Comparative measurements of activity of oxides of 32 chemical elements in
895 ketonization of propanoic acid," *Appl Catal A Gen*, vol. 470, pp. 278–284, Jan. 2014, doi:
896 10.1016/j.apcata.2013.10.047.

897 [12] Y. Yamada, M. Segawa, F. Sato, T. Kojima, and S. Sato, "Catalytic performance of rare earth
898 oxides in ketonization of acetic acid," *J Mol Catal A Chem*, vol. 346, no. 1–2, pp. 79–86, Jul.
899 2011, doi: 10.1016/j.molcata.2011.06.011.

900 [13] M. A. Hasan, M. I. Zaki, and L. Pasupulety, "Oxide-catalyzed conversion of acetic acid into
901 acetone: an FTIR spectroscopic investigation," *Appl Catal A Gen*, vol. 243, pp. 81–92, 2003.

[14] Y. Lee, J. W. Choi, D. J. Suh, J. M. Ha, and C. H. Lee, “Ketonization of hexanoic acid to diesel-blendable 6-undecanone on the stable zirconia aerogel catalyst,” *Appl Catal A Gen*, vol. 506, pp. 288–293, Oct. 2015, doi: 10.1016/j.apcata.2015.09.008.

[15] R. Kumar, N. Enjamuri, S. Shah, A. S. Al-Fatesh, J. J. Bravo-Suárez, and B. Chowdhury, “Ketonization of oxygenated hydrocarbons on metal oxide based catalysts,” *Catal Today*, vol. 302, pp. 16–49, Mar. 2018, doi: 10.1016/j.cattod.2017.09.044.

[16] S. Wang and E. Iglesia, “Experimental and Theoretical Evidence for the Reactivity of Bound Intermediates in Ketonization of Carboxylic Acids and Consequences of Acid-Base Properties of Oxide Catalysts,” *Journal of Physical Chemistry C*, vol. 121, no. 33, pp. 18030–18046, Aug. 2017, doi: 10.1021/acs.jpcc.7b05987.

[17] A. Ekman and P. Börjesson, “Environmental assessment of propionic acid produced in an agricultural biomass-based biorefinery system,” *J Clean Prod*, vol. 19, no. 11, pp. 1257–1265, Jul. 2011, doi: 10.1016/j.jclepro.2011.03.008.

[18] A. M. Abdel-Azeem, F. A. Abo Nouh, S. A. Gezaf, A. M. G. Darwish, and M. A. Abdel-Azeem, “Propionic acid chemistry and production,” in *Valorization of Biomass to Bioproducts*, Elsevier, 2023, pp. 3–15. doi: 10.1016/B978-0-12-822888-3.00011-6.

[19] B. Karasu and M. Cable, “The chemical durability of SrO–MgO–ZrO2–SiO2 glasses in strongly alkaline environments,” *J Eur Ceram Soc*, vol. 20, no. 14–15, pp. 2499–2508, Dec. 2000, doi: 10.1016/S0955-2219(00)00155-2.

[20] J. A. Onwudili, V. Sharma, C. A. Scaldaferri, and A. K. Hossain, “Production of upgraded fuel blend from fast pyrolysis bio-oil and organic solvent using a novel three-stage catalytic process and its combustion characteristics in a diesel engine,” *Fuel*, vol. 335, no. November 2022, p. 127028, 2023, doi: 10.1016/j.fuel.2022.127028.

[21] H. Bayahia, E. Kozhevnikova, and I. Kozhevnikov, “High catalytic activity of silicalite in gas-phase ketonisation of propionic acid,” *Chemical Communications*, vol. 49, no. 37, pp. 3842–3844, Apr. 2013, doi: 10.1039/c3cc41161c.

[22] J. A. Onwudili, I. Razaq, and K. E. Simons, “Optimisation of Propane Production from Hydrothermal Decarboxylation of Butyric Acid Using Pt/C Catalyst: Influence of Gaseous Reaction Atmospheres,” *Energies (Basel)*, vol. 15, no. 1, p. 268, Jan. 2022, doi: 10.3390/en15010268.

[23] R. W. Snell and B. H. Shanks, “CeMOx-promoted ketonization of biomass-derived carboxylic acids in the condensed phase,” *ACS Catal*, vol. 4, no. 2, pp. 512–518, Feb. 2014, doi: 10.1021/cs400851j.

[24] S. Wang and E. Iglesia, “Experimental and theoretical assessment of the mechanism and site requirements for ketonization of carboxylic acids on oxides,” *J Catal*, vol. 345, pp. 183–206, Jan. 2017, doi: 10.1016/j.jcat.2016.11.006.

[25] T. Viinikainen *et al.*, “Acidic and basic surface sites of zirconia-based biomass gasification gas clean-up catalysts,” *Appl Catal A Gen*, vol. 362, no. 1–2, pp. 169–177, Jun. 2009, doi: 10.1016/j.apcata.2009.04.037.

941 [26] Y. Guo *et al.*, “CeO2 Facet-Dependent Surface Reactive Intermediates and Activity during
942 Ketonization of Propionic Acid,” *ACS Catal*, vol. 12, no. 5, pp. 2998–3012, Mar. 2022, doi:
943 10.1021/acscatal.1c05994.

944 [27] T. N. Pham, D. Shi, and D. E. Resasco, “Reaction kinetics and mechanism of ketonization of
945 aliphatic carboxylic acids with different carbon chain lengths over Ru/TiO2 catalyst,” *J Catal*,
946 vol. 314, pp. 149–158, 2014, doi: 10.1016/j.jcat.2014.04.008.

947 [28] Z. Yang, Q. Yu, H. Wang, Q. Ge, and X. Zhu, “Ketonization of propionic acid over TS-1 and Ti-
948 Beta zeolites: Mechanism and effects of topology and hydrophobicity,” *J Catal*, vol. 429, p.
949 115247, Jan. 2024, doi: 10.1016/j.jcat.2023.115247.

950 [29] S. A. Aleem *et al.*, “Catalytic ketonization of palmitic acid over a series of transition metal
951 oxides supported on zirconia oxide-based catalysts,” *RSC Adv*, vol. 11, no. 51, pp. 31972–
952 31982, Aug. 2021, doi: 10.1039/d0ra10963k.

953 [30] T. Kulik, B. Palianytsia, and M. Larsson, “Catalytic pyrolysis of aliphatic carboxylic acids into
954 symmetric ketones over ceria-based catalysts: Kinetics, isotope effect and mechanism,”
955 *Catalysts*, vol. 10, no. 2, p. 179, Feb. 2020, doi: 10.3390/catal10020179.

956 [31] R. Pestman, R. M. Koster, A. Van Duijne, J. A. Z. Pieterse, and V. Ponec, “Reactions of
957 Carboxylic Acids on Oxides 2. Bimolecular Reaction of Aliphatic Acids to Ketones,” *J Catal*, vol.
958 168, pp. 265–272, 1997.

959 [32] E. Verkama, S. Albersberger, K. Meinander, M. Tiitta, R. Karinen, and R. L. Puurunen,
960 “Zirconia-Supported Pt, Pd, Rh, Ru, and Ni Catalysts in the Hydrotreatment of Fatty Amides
961 and Amines,” *Energy and Fuels*, vol. 38, no. 5, pp. 4464–4479, Mar. 2024, doi:
962 10.1021/acs.energyfuels.3c04372.

963 [33] E. I. Kauppi, K. Honkala, A. O. I. Krause, J. M. Kanervo, and L. Lefferts, “ZrO2 Acting as a Redox
964 Catalyst,” *Top Catal*, vol. 59, no. 8–9, pp. 823–832, May 2016, doi: 10.1007/s11244-016-0556-
965 4.

966 [34] M. Kogler *et al.*, “Hydrogen Surface Reactions and Adsorption Studied on Y2O3, YSZ, and
967 ZrO2,” *The Journal of Physical Chemistry C*, vol. 118, no. 16, pp. 8435–8444, Apr. 2014, doi:
968 10.1021/jp5008472.

969 [35] S. Tosoni and G. Pacchioni, “Acetic acid ketonization on tetragonal zirconia: Role of surface
970 reduction,” *J Catal*, vol. 344, pp. 465–473, Dec. 2016, doi: 10.1016/j.jcat.2016.10.002.

971 [36] S. Tosoni, H. Y. T. Chen, and G. Pacchioni, “A DFT study of Ni clusters deposition on titania and
972 zirconia (101) surfaces,” *Surf Sci*, vol. 646, pp. 230–238, Apr. 2016, doi:
973 10.1016/j.susc.2015.04.004.

974 [37] A. A. Shutilov, M. N. Simonov, Y. A. Zaytseva, G. A. Zenkovets, and I. L. Simakova, “Phase
975 composition and catalytic properties of ZrO2 and CeO 2-ZrO2 in the ketonization of pentanoic
976 acid to 5-nonanone,” *Kinetics and Catalysis*, vol. 54, no. 2, pp. 184–192, Mar. 2013, doi:
977 10.1134/S0023158413020134.

978 [38] Y. A. Zaytseva *et al.*, “Effect of gas atmosphere on catalytic behaviour of zirconia, ceria and
979 ceria-zirconia catalysts in valeric acid ketonization,” *Top Catal*, vol. 56, no. 9–10, pp. 846–855,
980 Jun. 2013, doi: 10.1007/s11244-013-0045-y.

[39] E. E. Farah, " Liquid Phase Ketonization of Pentanoic Acid into 5-Nonanone," Master of Science, American University of Beirut, Beirut, 2018.

[40] E. Karimi *et al.*, "Ketonization and deoxygenation of alkanoic acids and conversion of levulinic acid to hydrocarbons using a Red Mud bauxite mining waste as the catalyst," *Catal Today*, vol. 190, no. 1, pp. 73–88, Aug. 2012, doi: 10.1016/j.cattod.2011.11.028.

[41] K. Wu, M. Yang, W. Pu, Y. Wu, Y. Shi, and H. Hu, "Carbon Promoted ZrO_2 Catalysts for Aqueous-Phase Ketonization of Acetic Acid," *ACS Sustain Chem Eng*, vol. 5, no. 4, pp. 3509–3516, Apr. 2017, doi: 10.1021/acssuschemeng.7b00226.

[42] A. Hart, J. A. Onwudili, E. Yildirir, and S. E. Hashemnezhad, "Energy-dense sustainable aviation fuel-range hydrocarbons from cyclohexanone as a biomass-derived feedstock via sequential catalytic aldol condensation and hydrodeoxygenation," *Chemical Engineering Journal*, vol. 509, p. 161494, Apr. 2025, doi: 10.1016/j.cej.2025.161494.

[43] A. M. Lawal, A. Hart, H. Daly, C. Hardacre, and J. Wood, "Catalytic Hydrogenation of Short Chain Carboxylic Acids Typical of Model Compound Found in Bio-Oils," *Ind Eng Chem Res*, vol. 58, no. 19, p. 7998−8008, 2019, doi: 10.1021/acs.iecr.9b01093.

[44] S. T. Almutairi, E. F. Kozhevnikova, and I. V. Kozhevnikov, "Ketonisation of acetic acid on metal oxides: Catalyst activity, stability and mechanistic insights," *Appl Catal A Gen*, vol. 565, pp. 135–145, Sep. 2018, doi: 10.1016/j.apcata.2018.08.008.

[45] J. A. Bennett *et al.*, "Acetic Acid Ketonization over Fe3O4/SiO2 for Pyrolysis Bio-Oil Upgrading," *ChemCatChem*, vol. 9, no. 9, pp. 1648–1654, May 2017, doi: 10.1002/cctc.201601269.

[46] B. Boekaerts, W. Lorenz, J. Van Aelst, and B. F. Sels, "Kinetics of fatty acid ketonization in liquid phase with anatase and rutile TiO2 catalysts," *Appl Catal B*, vol. 305, p. 121052, May 2022, doi: 10.1016/j.apcatb.2021.121052.

[47] J. Jiao *et al.*, "Coke deposition mechanisms of propane dehydrogenation on different sites of Al_2O_3 supported PtSn catalysts," *Chemical Synthesis*, vol. 5, no. 1, Jan. 2025, doi: 10.20517/cs.2024.43.

[48] I.-H. Choi, H.-J. Lee, and K.-R. Hwang, "Understanding the effect of co-reactants on ketonization of carboxylic acids in the aqueous-phase pyrolysis oil of wood," *Wood Sci Technol*, vol. 55, no. 6, pp. 1745–1764, Nov. 2021, doi: 10.1007/s00226-021-01333-2.

[49] M. M. Hosseini, E. Kolvari, N. Koukabi, M. Ziyaei, and M. A. Zolfigol, "Zirconia Sulfuric Acid: An Efficient Heterogeneous Catalyst for the One-Pot Synthesis of 3,4-Dihydropyrimidinones Under Solvent-Free Conditions," *Catal Letters*, vol. 146, no. 6, pp. 1040–1049, Jun. 2016, doi: 10.1007/s10562-016-1723-8.

[50] D. Manoharan, A. Loganathan, V. Kurapati, and V. J. Nesamony, "Unique sharp photoluminescence of size-controlled sonochemically synthesized zirconia nanoparticles," *Ultrason Sonochem*, vol. 23, pp. 174–184, 2015, doi: 10.1016/j.ultsonch.2014.10.004.

[51] N. J. A. Rahman, A. Ramli, K. Jumbri, and Y. Uemura, "Tailoring the surface area and the acid–base properties of ZrO2 for biodiesel production from Nannochloropsis sp.," *Sci Rep*, vol. 9, no. 1, Dec. 2019, doi: 10.1038/s41598-019-52771-9.

[52] F. Ouyang, A. Nakayama, K. Tabada, and E. Suzuki, “Infrared Study of a Novel Acid - Base Site on ZrO2 by Adsorbed Probe Molecules. I. Pyridine, Carbon Dioxide, and Formic Acid Adsorption,” *Journal of Physical Chemistry B*, vol. 104, no. 9, pp. 2012–2018, Mar. 2000, doi: 10.1021/jp992970i.

[53] E. V. Fufachev, B. M. Weckhuysen, and P. C. A. Bruijnincx, “Crystal Phase Effects on the Gas-Phase Ketonization of Small Carboxylic Acids over TiO2 Catalysts,” *ChemSusChem*, vol. 14, no. 13, pp. 2710–2720, Jul. 2021, doi: 10.1002/cssc.202100721.

[54] S. Ding, J. Zhao, and Q. Yu, “Effect of zirconia polymorph on vapor-phase ketonization of propionic acid,” *Catalysts*, vol. 9, no. 9, p. 768, Sep. 2019, doi: 10.3390/catal9090768.

[55] D.-C. Lv, K. Jiang, K. Li, Y.-Q. Liu, D. Wang, and Y.-Y. Ye, “Effective suppression of coke formation with lignin-derived oil during the upgrading of pyrolysis oils,” *Biomass Bioenergy*, vol. 159, p. 106425, Apr. 2022, doi: 10.1016/j.biombioe.2022.106425.

Declaration of interests

▪ The authors declare that they have no known competing financial interests or personal relationships that could have appeared to influence the work reported in this paper.